

AMERICAN UNIVERSITY OF BEIRUT

EFFECT OF RESISTIVITY IN THE PROCESS OF
MAGNETIC RECONNECTION

by

FATIMA SAFIEDDINE

A thesis
submitted in partial fulfillment of the requirements
for the degree of Master of Science
to the Department of Physics
of the Faculty of Arts and Sciences
at the American University of Beirut

Beirut, Lebanon
December 2017

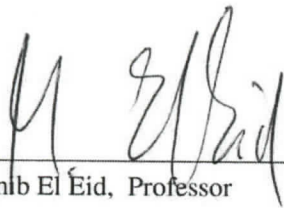
AMERICAN UNIVERSITY OF BEIRUT

EFFECT OF RESISTIVITY IN THE PROCESS OF
MAGNETIC RECONNECTION

by

FATIMA SAFIEDDINE

Approved by:



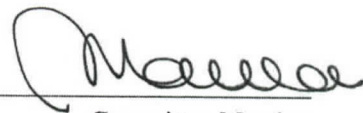
Dr. Mounib El Éid, Professor
Physics

Advisor



Dr. Michel Kazan, Professor
Physics

Committee Member



Dr. Marwan Darwish, Professor
Mechanical Engineering

Committee Member

Date of thesis defense: November 23, 2017

AMERICAN UNIVERSITY OF BEIRUT

THESIS, DISSERTATION, PROJECT RELEASE FORM

Student Name: Saieddine Fatima Hashem
Last First Middle

Master's Thesis Master's Project Doctoral Dissertation

I authorize the American University of Beirut to: (a) reproduce hard or electronic copies of my thesis, dissertation, or project; (b) include such copies in the archives and digital repositories of the University; and (c) make freely available such copies to third parties for research or educational purposes.

I authorize the American University of Beirut, to: (a) reproduce hard or electronic copies of it; (b) include such copies in the archives and digital repositories of the University; and (c) make freely available such copies to third parties for research or educational purposes after : **One --- year from the date of submission of my thesis, dissertation, or project.**
Two --- years from the date of submission of my thesis, dissertation, or project.
Three --- years from the date of submission of my thesis, dissertation, or project.

Fatima

22/2/2018

Signature

Date

This form is signed when submitting the thesis, dissertation, or project to the University Libraries

ACKNOWLEDGEMENTS

A thesis project is built in an environment of support and motivation. A big gratitude to my advisor, Prof. Mounib El-Eid, for his utmost supervision and care. His motivation have provided me with the continuous push forward and forward in thesis research.

I would like to thank my committee members, Prof. Marwan Darwish and Prof. Michel Kazan for their encouragement.

A special thanks to Prof. Marwan Darwish for all the discussions and time he spent sharing his knowledge and helping to complete my thesis.

Further thanks to Prof. Michel Kazan for his constructive comments and his essential support throughout the work.

Above all, I must express my very profound gratitude to my parents brothers and to my husband, for providing me with unfailing support and continuous encouragement throughout my years of study and through the process of researching and writing this thesis. This accomplishment would not have been possible without them. Thank you..

Finally, I would like to thank Mr. Mostafa Hammoud for his time and support. Every result described in this thesis was accomplished with the help and support of him. I greatly benefited from his keen scientific and numerical insight during the period it took to finalize the thesis.

AN ABSTRACT OF THE THESIS OF

Fatima Safieddine for Master of Science
Major: Physics

Title: Effect of Resistivity in the Process of Magnetic Reconnection

In this thesis, we will deal with an active area of theoretical research in astrophysical plasma physics, namely with the so called magnetic reconnection (MGR). This phenomenon is important from microphysics point of view, and from the wide range of its applications. The description of MGR is done in the frame work of the magnetohydrodynamics (briefly: MHD). However it cannot be initiated without including a mechanism of dissipation or resistivity. Applying the resistive MHD approach to MGR is a challenging task but it is worth doing, since MGR is important for understanding several phenomena, in particular solar flares, heating of the solar corona from which the solar wind originates. In addition, MGR plays a decisive role in understanding the interaction of the solar wind with the Earth's magnetosphere leading to geomagnetic storms, and to the formation of the auroras. In this work, we explore the effect of resistivity leading to dissipation and to the creation of a diffusive region in which a tremendous magnetic energy is released. While the present approach does not describe the MGR consistently, it is aim at illustrating the role of resistivity in the whole process of MGR. For this aim we show many results of modern numerical simulations which are unavoidable, since analytical solutions of the MHD equations are not possible. We show that MGR process takes place only if resistivity exists. However, resistivity does not seem to be effective when its constant through time and space. We then show through studying basic physical variables that contribute in MGR that increasing resistivity and changing dimensions of initial current sheet accelerates reconnection of magnetic field lines inside the diffusion region, so fast reconnection mechanism can be realized. Conversion of magnetic energy to heat and kinetic energy is also demonstrated leading to acceleration and heating of solar plasma particles.

CONTENTS

	Page
ACKNOWLEDGEMENTS	v
ABSTRACT	vi
I. General Overview	1
A. Introduction	1
B. Four Mysteries of MGR	3
C. Null points and Current sheets	6
D. Some observational evidence of Magnetic Reconnection	8
II. Physical Background of Magnetic Reconnection	10
A. Magnetohydrodynamics (MHD)	10
B. MHD Equations	11
1. Continuity equation	11
2. Momentum balance Equation	12
3. Induction Equation	13
4. Energy Equation and Gas Law	15
C. Ideal versus Non-Ideal MHD	17
D. Basic MGR models	17
1. Sweet-Parker Model	17
2. Petschek Model	19
E. Matching MGR to Observations	21
1. The Hall Effect	21

2. The Effect of Resistivity	22
III. Present Calculations of MGR	23
A. Numerical Method	23
B. Initial and Boundary Conditions	24
C. Accuracy of the Numerical Program	25
D. Numerical Computations	26
E. Results of the Present Calculations	27
1. Evolution of the Magnetic Field	27
2. Evolution of the Plasma Velocity	31
3. Evolution of the Plasma Density	32
4. Evolution of Magnetic Energy, Temperature and Kinetic Energy	36
5. Evolution of Reynold Number	38
6. The Rate of Magnetic Reconnection Process	39
7. Effect of the size of the current sheet	40
8. Effect of the initial Temperature	41
F. Observations	43
IV. Conclusion and Future Work	45

CHAPTER I

GENERAL OVERVIEW

A. Introduction

The plasma state is common and constitutes about 99 % of visible matter in the universe, and is considered to be the fourth fundamental state of matter besides the solid, liquid and gas states. Plasma exist in systems in which sufficient energy is provided at high temperatures to free electrons from their molecules and atoms keeping separate electrons and ions and leaving the plasma electrically neutral. This plasma state is distinguished from other matter states, because of the dominance of the electromagnetic interaction.

An interesting aspect of the astrophysical plasma, which we deal with in the present work is that space plasma provides the only possibility of testing processes which are thought to take place in a plasma but not accessible to lab measurements. In this respect, the Sun is a cosmic laboratory for studying basic properties of a plasma. An important plasma process is the magnetic reconnection (briefly: MGR). This process is a fundamental dynamical process in highly conductive plasma. It is considered to be a key process in releasing tremendous amount of magnetic energy, and is thought to lead to several Sun remarkable activities, such as:

- Solar flares and prominence,
- Heating of solar corona from which the solar wind emerges,
- Understanding the interaction between the solar wind and the Earth magnetosphere.
- A large amount of experimental evidence for MGR if also found in toroidal fusion devices such as Tokomaks, where toroidal currents are induced to heat the plasma and produce poloidal magnetic fields.

In the following we summarize the basic concept of MGR in order to illustrate the scope of our project. The phenomena outlined above represent huge explosion events in which

a tremendous amount of magnetic energy is released. Then, the question is how magnetic fields release such energies. The answer will sound simple but the subject is very complex.

Simple is that adjacent magnetic fields pointing in opposite directions tend to annihilate each other releasing their magnetic energy and heating the charged particles in the surrounding.

Complex and astonishing is that the time required for such annihilation is about 10,000 years for the Sun's corona, while observed energy released times from magnetic explosion are only hundreds of seconds. This extremely fast release of energy is linked to MGR. Even though, this idea was suggested relatively long time ago [1], it remains to date only partially understood. It is because modern numerical simulation with the fastest computers are required as we shall see below.

The basic idea about MGR was suggested by H. Petschek [2], the so called (fast reconnection). Then J. Dungey [3] suggested that neutral points, where the magnetic fields pointing in opposite direction can annihilate one another releasing energy through MGR. Suppose two plasmas containing magnetic fields with opposite directions are separated by a thin boundary as seen in (Fig. 1a). If by some means the adjacent field cross the boundary, or becomes reconnected (Fig. 1b), then the field pointing downward is now connected with the field pointing upward. Consequently, the resulting bent field has tension like a rubber band. The behavior of the magnetic field with the plasma is like two back-to-back slingshots (Fig. 1c). But, the magnetic field accelerates the plasma away from the reconnection region and releases magnetic energy.

The new fields coming from the sides are now ready to reconnect and release their energy. It is actually an explosive release of magnetic energy, which is self-driven. Notice that in traditional explosion, the blast wave is the same in all directions, but during MGR high-speed flow is only upward or downward and the plasma flows slowly from the other directions (see Fig. 1c).

An exciting question is: what would cause magnetic field to reconnect? The two oppo-

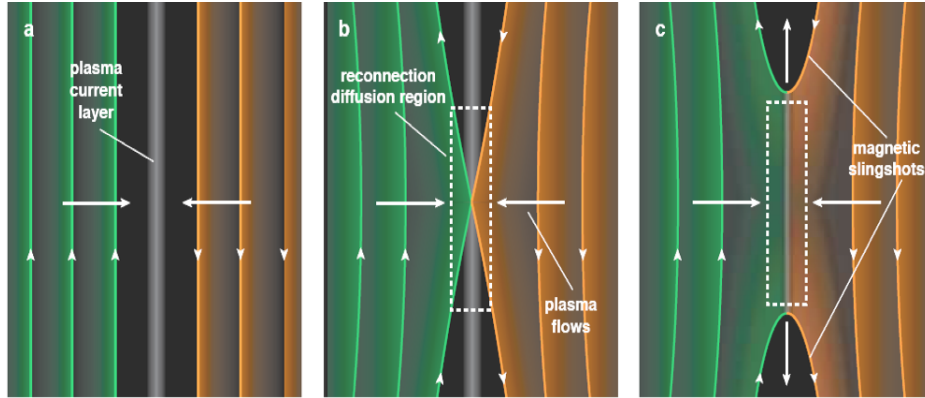


Figure 1: Magnetic Reconnection, see text for explanation

sitely directed fields must be separated by an electrical current directed inward within the boundary between them. Also an electric field pointing into the page is a necessary ingredient. This field parallel to the current leads to dissipation of electrical energy into thermal energy like in an electric circuit. Then, it is the dissipation which leads to the MGR.

In Figs. 1b, 1c, the boxes indicate the region of diffusion where the magnetic dissipation occurs. Thus, outside the box the magnetic field is frozen in the plasma, but within the box the frozen-in condition breaks down because of dissipation, so that the field can reconnect.

B. Four Mysteries of MGR

It is interesting to describe four mysteries which all are related to magnetic reconnection. They are shortly described as follows

First Mystery

The plasma can regarded collision-less even on the region of diffusion. What causes then the dissipation? This is the first mystery . The answer seems to be connected to the shape of the diffusion region, or its aspect ratio (width over length), which controls the rate of

release of magnetic energy. It seems that a narrow region promote the energy release. This will be illustrated and confirmed in Section E-7 in ChII.

Second Mystery

A second mystery of MGR is the question what determines the aspect ratio of the dissipation region and the rate of release of magnetic energy.

Third Mystery

MGR often occurs as a flare explosion (similar to the solar flares), but the magnetic energy builds up over a long period of time and is suddenly released . Why doesn't the magnetic energy simply dissipates at the same rate at which it has been generated. The third mystery is: does the sudden increase of dissipation set off reconnection?

Fourth Mystery

Observations have shown that particles are accelerated in MGR. But, the acceleration mechanism cannot be explained through classical fluid dynamics. The fourth mystery concerns the efficient mechanism of converting magnetic energy into kinetic energy of the particles.

Understanding these mysteries requires fast computers which are available now.

Theoretical Insight

Computer simulations have, for the first time, enabled real comparison with observations. In the following, a brief summary is given about certain achievement in understanding MGR which is useful in connection with the present work.

The first mystery described above, namely that the classical electron-ion collision as first was proposed by Sweet and Parker [1] does not lead to sufficient dissipation to explain the explosive release of magnetic energy.

The first mystery was to replace classical resistivity in collision-less plasma. The intense current produced during MGR generates turbulent electric-field fluctuations that scatter electrons. The electrons gain energy from the magnetic field producing an **anomalous resistivity**. That is, with turbulence the field lines would be strongly twisted so that many of them would reconnect enforcing the reconnection rate. It is clear that numerical simulation is at place here, and this has to wait 20 years waiting for fast computers.

So far, the learn effect from the simulations is that the transition from classical resistivity to anomalous resistivity takes place when the diffusion region thins down, and turbulence plays a major role.

Concerning the second mystery, about what controls the energy release, a major insight has been achieved, see [4] for more details. The ions and electrons, because of their different masses would move differently at small spatial scales of the diffusion region. The ion motion can be neglected at small scale. Freed from the ions, the electrons together with the embedded magnetic field can flow at very high velocity. The result from a flurry of papers has shown that the rate of reconnection increases dramatically and contradicts the former view based on the Sweet-Parker model that this rate was controlled by the ions and the electrons.

The key feature was that a "Hall Reconnection". It is that a Hall magnetic field develops as a result of the relative motion of the electrons and ions in the reconnection diffusive region. The amazing thing is that the structure of the Hall magnetic field has been documented in magnetospheric satellite observations.

An interesting example of magnetic reconnection is the interaction of the Solar wind with the Earth's magnetosphere. Fig. 2 below shows the intergalactic magnetic field carried by the solar wind and pointing southward (yellow color) facing the geomagnetic magnetic field lines emanating from the Earth pointing northward (green color) at the side of the Earth facing the Sun.

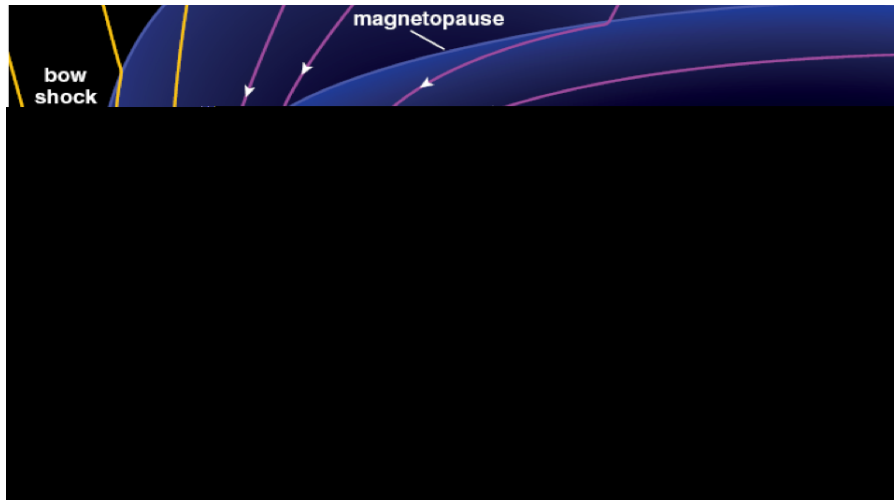


Figure 2: Magnetic reconnection in Earth Magnetosphere

The dashed box on the left shows the region of magnetic reconnection. This reconnection allows the charged particles and energy to enter the magnetosphere.

Another dashed box on the right shows a second region of reconnection where northern and southern magnetic lines reconnect. This is suggested to lead to the auroral activity or geomagnetic substorm. For this important process on Earth NASA has launched a mission called "MMS", see link below:

<http://mms.space.swri.edu/science-2.html>.

C. Null points and Current sheets

Null points are lines and surfaces of magnetic fields, and they serve as location where the magnetic field vanishes. The X-type points constitute the most important topological peculiarity of MGR. They are the places where redistribution of magnetic fluxes occurs, which changes the connectivity of field lines. They can occur whether the magnetized medium is conducting, as in plasma, or not, as in neutral gas. The simplest example is that of two parallel electric currents of equal magnitude in vacuum.

As seen in Fig. 3, the magnetic field of these currents forms three different fluxes in the

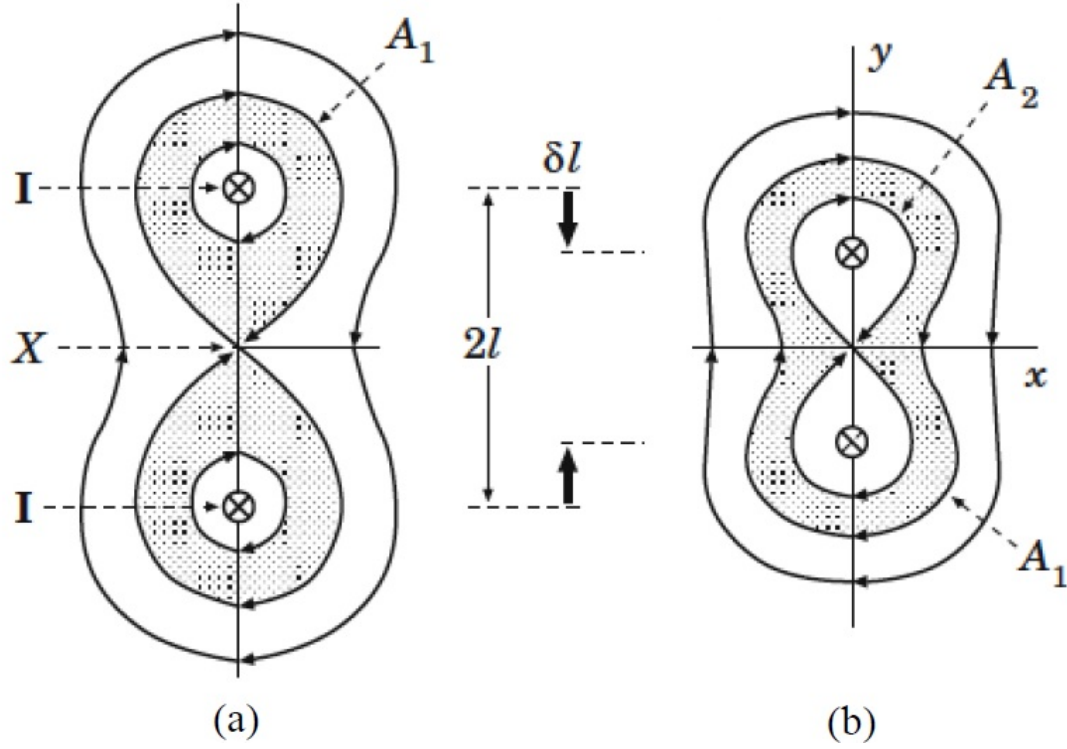


Figure 3: (a) Initial state, separatrix field line A_1 and (b) Final state, separatrix field line A_2

plane (x, y) . Two of them belong to the upper and lower currents respectively, and are situated inside the separatrix field line A_1 (See figure 3-a) that forms eight-like curve with a zeroth X-point. The third flux situated outside this curve belongs to both currents and it's found outside the separatrix region A_1 . If the currents are displaced in the direction of each other, then the following redistribution of magnetic flux will take place and the current's proper fluxes will diminish by a quantity δA , while their common flux will increase by the same quantity. So the field line A_2 will be the separatrix of the final state (See figure 3-b). This process is realized as follows, two field lines approach the X-point, merge, form separatrix, and then they reconnect forming a field line which encloses both currents. This is the process of reconnection of field lines with A_2 the last reconnected field line [2].

On the other hand, current sheets are a thin current carrying layer across which the magnetic field changes direction, magnitude or both. Unlike null points, they can only exist in conducting media. In plasmas, null points give rise to current sheets.

Current sheet naturally tends to diffuse away and convert magnetic energy into heat energy by Ohm's law. The field lines diffuse inwards through the plasma and cancel, so that the region of diffused field spreads out. Therefore a steady state may be produced if magnetic flux is carried in, with the plasma, at the same rate as it is trying to diffuse. If the resistivity is small, i.e. global magnetic Reynolds number is much greater than unity, then we have an extremely small length scale L , and therefore large magnetic gradient and current \mathbf{j} will be created. Furthermore, although the magnetic field may be destroyed by cancellation as it comes in, the plasma itself cannot be destroyed and has to flow sideways. This will be explained in the following.

D. Some observational evidence of Magnetic Reconnection

MGR is observed in space plasma and in plasma laboratories as well. In astrophysical environment, it is eventually an important mechanism in the process of star formation and formation of accretion disks around stellar objects. It seems that the liberation of huge solar energy through coronal mass ejection and prominence eruption. The existence of the Earth's magnetosphere is preventing the solar wind to reach the Earth's surface as it was illustrated in Fig (2).

We also mention that MGR seems to play an important role in the process of star formation and the formation of accretion disks around stellar objects [3,4]

MGR may provide a reasonable mechanism for the heating of the solar corona and it may be the cause of solar flares. It is considered to play a major role in the evolution of solar corona from which coronal mass ejections are emerging [2]. Solar flares have been central objects for studying physical mechanisms of MGR. The topologies of soft X-ray pictures are seen to change within a time scale of minutes or hours. The study of the dynamics of solar flares has been intensified through the detailed pictures of solar coronal activities. These pictures were recently taken by modern satellites from Skylab in the 1970's, Yohkoh, and in present times through Solar and Heliospheric Observatory

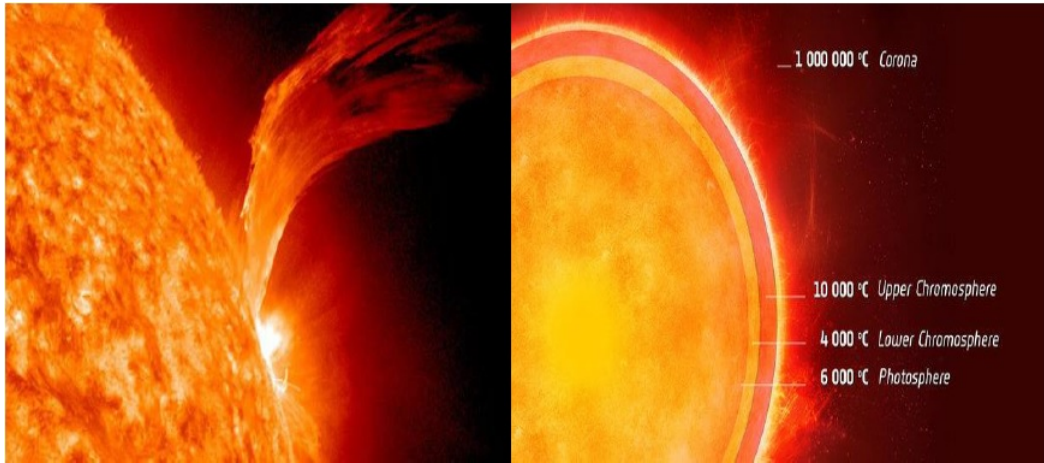


Figure 4: The solar flares

SOHO, TRACE, Ramaty high energy solar spectroscopic imager RHESSI, and Hinode. These satellites have revealed the solar atmosphere with unprecedented spatial and temporal resolution covering wave-lengths from ultraviolet through soft and hard X-rays to γ -rays. With many large coronal loops seen actively interacting with themselves (See figure 4), their topology is observed to change rapidly and may be largely related to as predicted by magnetic reconnection[2].

During magnetic reconnection, conversion of magnetic energy should occur in the solar upper atmosphere, where a much higher plasma temperature than that of the photosphere is routinely observed. Finding the true cause of heating of the corona to more than 10^6 kelvins is a major goal of solar plasma physics [1]. While there are other possibilities such as wave heating, reconnection is the most likely candidate for the coronal heating mechanism since the magnetic field represents the dominant energy source in the corona.

CHAPTER II

PHYSICAL BACKGROUND OF MAGNETIC RECONNECTION

A. Magnetohydrodynamics (MHD)

Since we treat MGR in the context of MHD, it is useful to describe what MHD is in principle. Terrestrial magnetic field is generated in the liquid outer core of the Earth's interior. Solar magnetic field generates sunspots and solar flares, and galactic magnetic field influences the star formation process in giant molecular clouds.

All these flows are studied in the framework of the MHD. MHD is described as mutual interaction of fluid flow and the magnetic field. The fluids must be electrically conducting and non-magnetic, and this is what is realized in a plasma being a hot ionized system. In other words there is a mutual interaction between the magnetic field \mathbf{B} and the fluid velocity \mathbf{u} . The difference between electrodynamics and MHD is the fluidity of the conductor. This is the reason why the interaction between \mathbf{B} and \mathbf{u} becomes rather complex as we will see in this work.

Useful parameters of MHD are the following:

-Magnetic Reynolds number

$$R_m = \frac{\mu d v}{\eta}$$

-Alfven velocity

$$v_A = \frac{B}{\sqrt{\rho \mu}}$$

-Lundquist number (Reynolds number with Alfven velocity)

$$S = \frac{d v_A}{\eta}$$

-Diffusion time

$$\tau_D = \frac{\mu_0 d^2}{\eta}$$

-Alfven time

$$\tau_A = \frac{d}{v_A}$$

Where μ the permeability of free space, σ the electrical conductivity, d is a scale length, u the fluid velocity and η is the resistivity .

The Reynolds number is a measure of conductivity, the others are self-explained. If R_m is large the magnetic field line will be frozen in into the conducting medium. If it is small, there will be little influence of u on B . In this case, the magnetic field is dissipative in nature, so that a damping mechanical motion will be converting kinetic energy into joule heating. This is what will be seen in the process of magnetic reconnection. The relevant time scale is the damping time τ .

B. MHD Equations

In this work, we describe MGR in a simplified model based on a single fluid approach, treating the ions and electrons together. It is beyond the scope of the present work to present more extended description such as two-fluid model. Our main focus will be to investigate the effect of dissipation on MGR as we will describe in chap.III. This description is based on the MHD equations, which we summarize in the following.

1. Continuity equation

The continuity equation describes the transport of some quantity. It is simple and particularly powerful when applied to a conserved quantity, but it can be generalized to apply to any extensive quantity. In this work we use only conserved quantities which are less oscillating in any numerical solution. The mathematical form of the continuity equation is given by,

$$\frac{\partial \rho}{\partial t} + \nabla(\rho \mathbf{U}) = 0 \quad (1)$$

Where ρ is the mass density and \mathbf{U} is the bulk plasma velocity. Physically, Eq. (1) is a scalar relation describing the time rate of change of plasma density of the given plasma element as it moves through space.

2. Momentum balance Equation

The momentum balance equation is the Newtons 2nd law applied to the moving plasma element. It means that the net force on the plasma element equals its mass times its acceleration. This is a vector relation, and hence can be split into three scalar relations along the x , y , and z -axes. The mathematical form of such equation is given by,

$$\frac{\partial(\rho \mathbf{U})}{\partial t} + \nabla \cdot (\rho \mathbf{U} \mathbf{U}) = -\nabla p + \mathbf{J} \times \mathbf{B} + \mathbf{F}_{viscosity} \quad (2)$$

where p is the plasma pressure, \mathbf{J} is the current density resulting from the motion of electrons and ions in the plasma and \mathbf{B} is the external magnetic field which governs the dynamics of both electrons and ions. The term $\mathbf{J} \times \mathbf{B}$ is the magnetic force namely the Lorentz force, while $\mathbf{F}_{viscosity}$ refers to viscous forces such as $\nu \Delta \mathbf{U}$ (ν is the dynamic viscosity expressed in kg/m.sec) and other dissipative forces. In our present treatment, all the dissipative forces refer to $\nu \Delta \mathbf{U}$ and all gravitational forces are neglected. Using the Ampere's law

$$\mathbf{J} = \frac{1}{\mu_0} \nabla \times \mathbf{B},$$

one can expand the Lorentz force as

$$\mathbf{J} \times \mathbf{B} = -\nabla \left(\frac{B^2}{2\mu_0} \right) + \nabla \cdot \left(\frac{\mathbf{B}\mathbf{B}}{\mu_0} \right).$$

Finally, the momentum balance equation in conservative form can then be written as

$$\frac{\partial(\rho\mathbf{U})}{\partial t} + \nabla \cdot (\rho\mathbf{U}\mathbf{U}) - \nu\Delta\mathbf{U} = -\nabla\left(p + \frac{B^2}{2\mu_0}\right) - \nabla\left(\frac{\mathbf{B}\mathbf{B}}{\mu_0}\right) \quad (3)$$

It should not be confused between B^2 and $\mathbf{B}\mathbf{B}$. B^2 is a scalar whereas $\mathbf{B}\mathbf{B}$ and $\rho\mathbf{U}\mathbf{U}$ are tensors of rank 3. The tensor $\mathbf{B}\mathbf{B}$ is obtained by the product of (3, 1)-by-(1, 3) vectors. In Eq. (3), the additional quantity to the pressure, $\frac{B^2}{2\mu_0}$, is known as the magnetic pressure or magnetic energy density.

3. Induction Equation

The Maxwell equations should be coupled to the plasma equations which is established by the Ohms law. The Ohms law states that the electric field seen in the moving frame of the plasma is proportional to the resistivity (η) times current density (\mathbf{J}), that is

$$\mathbf{E} + \mathbf{U} \times \mathbf{B} = \eta\mathbf{J}. \quad (4)$$

This is the simplest form of the Ohms law, the more general one includes correction like the Hall effect and electric pressure gradient. Furthermore, η is not always a scalar. The induction equation is obtained by substituting Ohm's law and Ampere's law into the Faraday's law

$$\frac{\partial\mathbf{B}}{\partial t} + \nabla(\mathbf{U}\mathbf{B}) - \frac{\eta}{\mu_0}\nabla^2\mathbf{B} = \nabla(\mathbf{B}\mathbf{U}) + \frac{1}{\mu_0}(\nabla \times \mathbf{B}) \times \nabla\eta \quad (5)$$

Note that η is not assumed constant in this equation. This will help to study its spacial variation as we will describe in chapter.III.

The induction equation can be written in terms of the Reynolds number as introduced above. The induction equation above with constant (η) can be written as:

$$\frac{\partial \mathbf{B}}{\partial t} = \nabla \times (\mathbf{U} \times \mathbf{B}) - \frac{\eta}{\mu_0} \cdot \nabla (\nabla \times \mathbf{B}).$$

When the magnetic fields, the distance scales and the velocities are normalized to typical values B_0 , d_0 and V_0 respectively, where B_0 is the original magnetic field, d_0 is the half-thickness of the initial current layer, and v_0 the Alfvén velocity in x-direction, and ρ_0 is initial plasma density with the time $t_0 = d_0/v_0$ the induction equation becomes:

$$\frac{(B_0)^2}{d_0 \sqrt{\mu_0 \rho_0}} \cdot \frac{\partial \tilde{\mathbf{B}}}{\partial \tilde{t}} = \frac{B_0^2}{d_0 \sqrt{\mu_0 \rho_0}} \tilde{\nabla} \times (\tilde{\mathbf{U}} \times \tilde{\mathbf{B}}) - \frac{\eta}{\mu_0} \frac{B_0}{(d_0)^2} \tilde{\nabla} (\tilde{\nabla} \times \tilde{\mathbf{B}})$$

In a final form, the induction equation can be written as

$$\frac{\partial \tilde{\mathbf{B}}}{\partial \tilde{t}} = \tilde{\nabla} \times (\tilde{\mathbf{U}} \times \tilde{\mathbf{B}}) - \frac{1}{R_m} \tilde{\nabla} (\tilde{\nabla} \times \tilde{\mathbf{B}}) \quad (6)$$

where the magnetic Reynold number is $R_m = \frac{d_0 V_0}{\eta / \mu_0}$. Physically, in fluids, the Reynold number is an experimental number used to predict the flow velocity at which turbulence will occur. It is described as the ratio of inertial forces to viscous forces. In plasma, this number represents the ratio of inertial forces to viscous forces coming from magnetic diffusivity η / μ_0 . MGR needs plasma not to be frozen-in the magnetic field lines, this happens in very thin current layers when magnetic viscous forces dominate the inertial forces i.e. $R_m < 1$. In other words, when resistivity becomes important, plasma particles start to escape from the field lines they hold to other field lines allowing MGR process to take place. However, in almost plasma systems, frozen-in condition is essential keeping $R_m \gg 1$, where plasma is perfectly conducting and magnetic field lines behave as if they move with the plasma.

4. Energy Equation and Gas Law

In a plasma, the energy equation can be stated as the rate of change of the energy density inside a plasma element, it is equal to the net flux of heat into the element plus the Rate of work done on the element due to body and surface forces. Like all the equations we have mentioned above, the energy equation can be presented in two forms, conservative and non-conservative. The basic form of the energy equation is

$$\frac{\partial p}{\partial t} + \mathbf{U} \cdot \nabla p + \gamma p \nabla \cdot \mathbf{U} = 0. \quad (7)$$

The plasma pressure can be related to the internal energy per unit mass e namely the gas law

$$p = (\gamma - 1)\rho e. \quad (8)$$

With the help of the gas law and the continuity equation, Eq. (1) and Eq. (8), one can have the energy equation in conservative form

$$\frac{\partial(\rho e)}{\partial t} + \nabla \cdot (\rho e \mathbf{U}) + p \nabla \cdot \mathbf{U} = 0. \quad (9)$$

Note that Eq. (9) evaluates only the variation of the internal energy per unit mass e . However; our plasma system includes other two forms of energy, the kinetic energy $\frac{1}{2}\rho U^2$ and the magnetic energy $\frac{B^2}{2\mu_0}$. Multiplying (2) by the plasma bulk velocity \mathbf{U} , provides an energy equation for the kinetic energy

$$\frac{\partial}{\partial t} \left(\frac{1}{2} \rho U^2 \right) + \nabla \cdot \left(\frac{1}{2} \rho U^2 \mathbf{U} \right) = -\mathbf{U} \cdot \nabla p + \mathbf{U} \cdot (\mathbf{J} \times \mathbf{B}) + \nu \mathbf{U} \cdot \Delta \mathbf{U}. \quad (10)$$

Similarly, the energy equation for magnetic energy is obtained by multiplying the magnetic field \mathbf{B} with the induction equation, Eq. (5), namely

$$\begin{aligned} \frac{\partial}{\partial t} \left(\frac{B^2}{2\mu_0} \right) + \nabla \cdot \left(\mathbf{B} \cdot \frac{\mathbf{B}\mathbf{U}}{\mu_0} - \mathbf{U} \cdot \frac{\mathbf{B}\mathbf{B}}{\mu_0} \right) &= -\mathbf{U} \cdot (\mathbf{J} \times \mathbf{B}) + \frac{\eta}{\mu_0^2} \mathbf{B} \cdot \nabla^2 \mathbf{B} \\ &+ \frac{1}{\mu_0^2} \mathbf{B} \cdot \left((\nabla \times \mathbf{B}) \times \nabla \eta \right) \end{aligned} \quad (11)$$

So far, Eqs. (9, 10, 11) are three different equations evaluating the internal, kinetic and magnetic energies respectively. By adding them up, one gets a very useful equation for the total energy E_{tot} of the plasma system we are dealing with in this work. In conservative form, this equation is

$$\begin{aligned} \frac{\partial E_{tot}}{\partial t} + \nabla \cdot (E_{tot} \mathbf{U}) &= -\nabla \cdot \left(\left(p + \frac{B^2}{2\mu_0} \right) \mathbf{U} \right) + \frac{1}{\mu_0} \mathbf{B} \cdot \nabla (\mathbf{U} \cdot \mathbf{B}) + \nu \mathbf{U} \cdot \Delta \mathbf{U} \\ &- \frac{\eta}{\mu_0} \left(\nabla \cdot \left(\nabla \cdot \left(\frac{\mathbf{B}\mathbf{B}}{\mu_0} \right) \right) - \Delta \left(\frac{B^2}{2\mu_0} \right) \right) \\ &- \frac{1}{\mu_0} \nabla \eta \cdot \left(\nabla \cdot \left(\frac{\mathbf{B}\mathbf{B}}{\mu_0} \right) - \nabla \left(\frac{B^2}{2\mu_0} \right) \right) + \text{Source Term} \end{aligned} \quad (12)$$

where the total energy is $E_{tot} = \rho e + \frac{1}{2} \rho U^2 + \frac{B^2}{2\mu_0}$. During MGR process, there is a noticeable change in temperature indicating that plasma is heated up. The excess amount of heat should be coming from the magnetic energy. For this sake, the energy equation must contain a source of heat which can be expressed as $\nabla \cdot (\kappa \nabla T)$, where κ is the thermal conductivity and T is the temperature.

C. Ideal versus Non-Ideal MHD

In astrophysical environments, the distinction between ideal and non-ideal process is important because simple estimates imply that magnetic dissipation acts on a time scale which is many orders of magnitude slower than the observed time scales of dynamic phenomena. For example, the solar flare releases stored magnetic energy in the corona within a period of 100 seconds. By comparison, the time scale for magnetic dissipation based on a global scale-length of 10^5 km is of order 10^6 years. Typically, phenomena like solar flares and substorms require significant fraction of the stored magnetic energy to be converted with a few Alfvén time scales. Such rapid time scales are easily achieved in ideal MHD processes but not in a non-ideal one. Although MGR processes are capable of releasing energy quickly, they rarely release a significant amount since there exist a topological constraints in the absence of dissipation. In contrast, magnetic reconnection is not topologically constrained, and hence much greater amount of magnetic energy is released through it [11].

In ideal MHD plasma, plasma and magnetic field line velocities have same order of magnitude and same direction as well. Using this approach, the magnetic energy is transformed to kinetic energy without heat dissipation, no significant amount of magnetic energy is released, and the time scale of the process is relatively fast.

D. Basic MGR models

1. Sweet-Parker Model

The Sweet-Parker model consists of a simple diffusion region of length $2L$ and width 2δ lying between oppositely directed magnetic fields \mathbf{B} of equal strength B (See figure 5). The system is two dimensional and steady-state. The induction equation for

(Sweet 1958; Parker 1957, 1963)

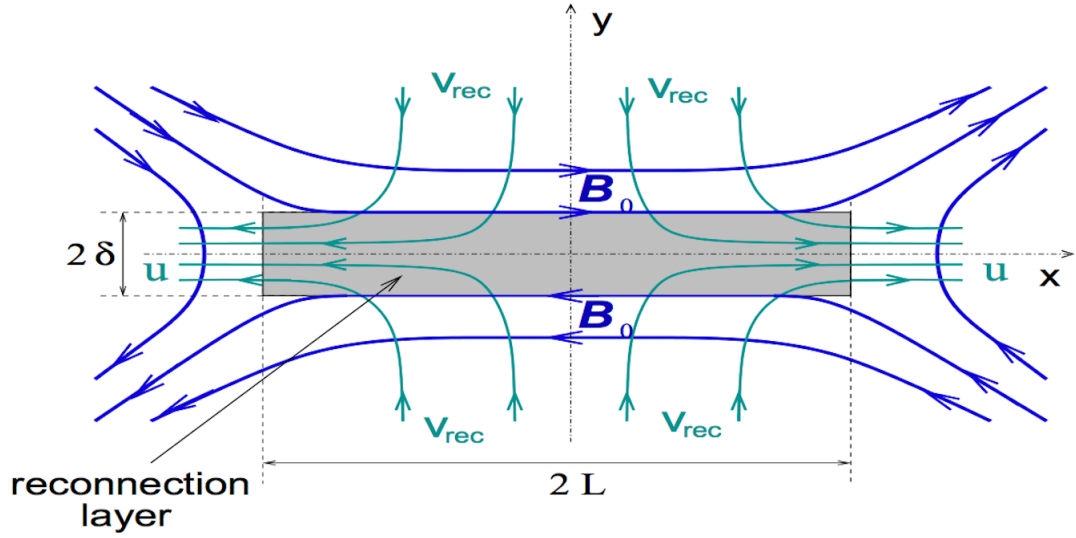


Figure 5: Sweet-Parker RCL

two-dimensional steady state integrates to Ohm's law:

$$\mathbf{E} + (\mathbf{v} \times \mathbf{B}) = \eta \mathbf{j} \quad (13)$$

where \mathbf{E} is the electric field normal to the xy -plane, in which the flow and the magnetic field lie.

Plasma is assumed to diffuse into the current layer, along its whole length, at some relatively small inflow velocity, v_i . The plasma is accelerated along the layer, and eventually expelled from its two ends at some relatively large exit velocity, v_o . The inflow velocity is simply an $\mathbf{E} \times \mathbf{B}$ velocity, so:

-Ohms law: $v_i B_o = E_z = \eta j = \eta \frac{B_o}{\delta}$, then $\eta = v_i \delta$

-Vertical pressure balance: $p(0,0) = p_0 + \frac{(B_o)^2}{8\pi}$

-Equation of motion: $\rho v_x \frac{\partial v_x}{\partial x} = -\frac{\partial P}{\partial x}$, then $u = v_A = \frac{B_o}{\sqrt{4\pi\rho}}$

-Mass Conservation: $v_i L = u \delta$

-Rate: $r = \frac{v_i}{v_A} = \frac{\delta}{L} = \frac{1}{\sqrt{R_m}}$

-Time scale: $\tau_{S-P} \sim \tau_A \sqrt{R_m}$

In Sweet-Parker mechanism, the sheet length L is identified with the global external length scale L_e . Therefore magnetic Reynolds number is $R_m = \frac{L_e v_A}{\eta} \gg 1$.

The Sweet-Parker reconnection is undoubtedly correct. It has been simulated numerically innumerable times, and was recently confirmed experimentally in the Magnetic Reconnection Experiment (MRX) operated by Princeton Plasma Physics Laboratory.[6] The problem is that Sweet-Parker reconnection takes place far too slowly to account for many reconnection processes which are thought to take place in the solar system. For instance, in solar flares using the typical values:

$L \approx 10^5$ km, $\rho \approx 10^{-14}$ g/cm³, $B \approx 100$ G, $T \approx 10^7$ kelvins, we find $n \approx 2.5 \times 10^9$ cm⁻³, $v_A \approx 3 \times 10^8$ cm/s and $\tau_e \approx 10$ sec, where the electron collision time is estimated from Braginskii(1965). [6]

Considering Ohmic resistivity, we can then find:

$$\eta = \frac{c^2 m_e}{4\pi n_e^2 \tau_e} \approx 10^{10} \text{ cm}^2/\text{sec}.$$

Then $R_m \approx 10^{17}$, and we have $l \approx 30$ cm, so we got the Sweet-Parker time scale as:

$$\tau_{SP} = \sqrt{R_m} \frac{L}{v_A} \approx 10^{10} \text{ s}.$$

However, the observed time-scale of the solar flare is of order 10^4 sec [12], which is 6 orders of magnitude smaller than the Sweet-Parker model predictions.

2. *Petschek Model*

Because of such an enormous gap between the diffusion time and the Alfvén time, not only laboratory experiments but also numerical experiments with realistic magnetic Reynolds numbers ($R_m = \frac{v_D}{\tau_A}$) are still impossible. This is why the magnetic reconnection model has not been yet fully established. In order to solve this fundamental question, several important studies have been done till now.

Resolution of this problem was suggested by Petschek.[13] Petschek (1964) pointed

out that, since the magnetic reconnection was a topological process, the field lines need not reconnect along the entire length ($2L$) of the boundary layer, but could merge over a shorter length (2Δ) (See figure 7). For this to happen, he suggested that the rest of the boundary layer region should consist of slow shocks which could accelerate the matter that did not pass through the diffusion region and that magnetic energy can be converted into plasma thermal energy as a result of shock waves being set up in the plasma, in addition to the conversion due to the action of resistive diffusion.[13] It must be pointed out that the Petschek model is very controversial. Many physicists think that it is completely wrong, and that the maximum rate of magnetic reconnection allowed by MHD is that predicted by the Sweet-Parker model. Although his model increased rate of reconnection to a factor of $\sqrt{\frac{L}{\Delta}}$ faster than the Sweet-Parker reconnection velocity [13] but still the most powerful argument against the validity of the Petschek model is the fact that, more than 30 years after it was first proposed, nobody has ever managed to simulate Petschek reconnection numerically [11].

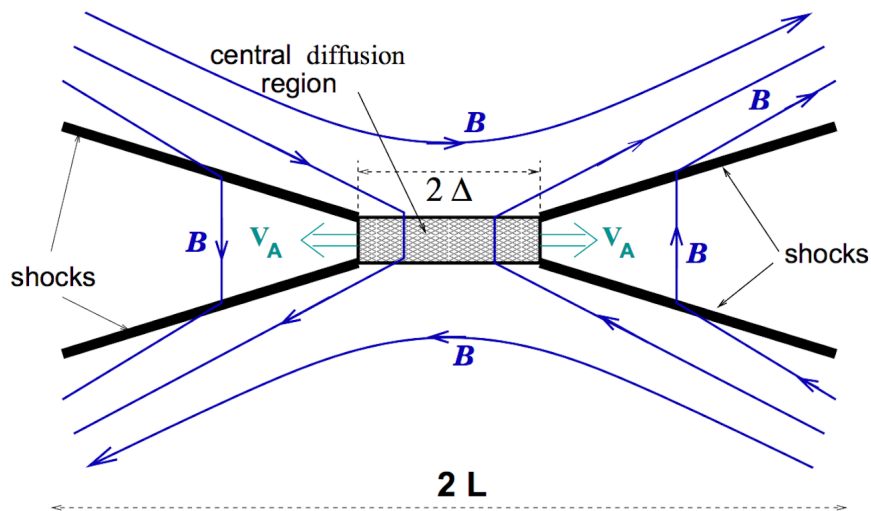


Figure 6: Petschek RCL

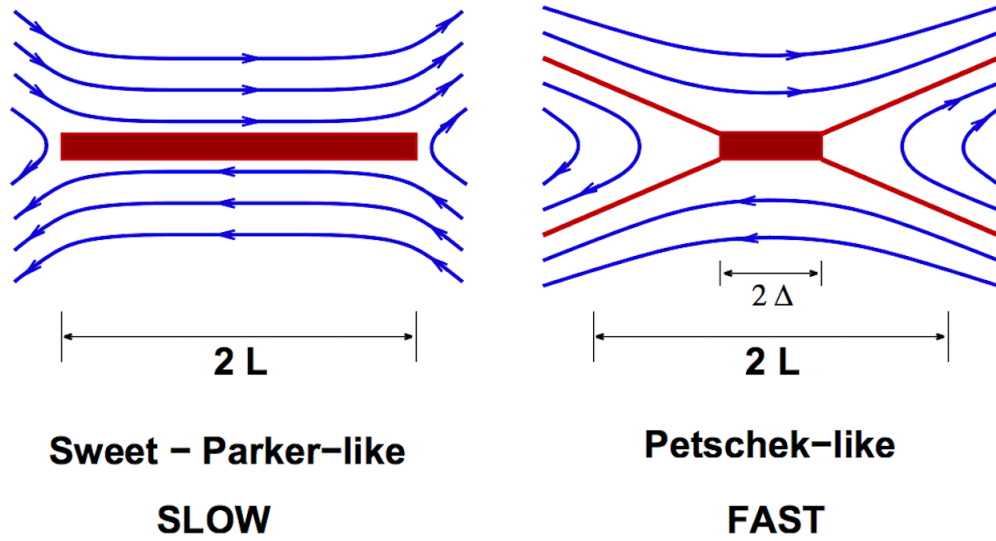


Figure 7: Difference between Sweet-Parker and Petschek geometry.

E. Matching MGR to Observations

Sweet-Parker and Petschek models are considered as two models lacking of complete description of MGR. It seems now that different computational models should be considered to possibly match the observations. The most important publications set after Petschek and Parker were Biskamp (1986); Ma and Bhattacharjee (1996); Uzdensky and Kulsrud (1998, 2000); Breslau and Jardin (2003); Malyshkin et al. (2005) [6]. They all set two candidates that can hold to solve a better model for reconnection, namely the Hall effect and the effect of resistivity.

1. *The Hall Effect*

Hall-MHD reconnection involves two-fluid laminar configuration. As mentioned above, magnetic reconnection was described primarily through the MHD theory which was developed in the early phase of the plasma research, treating the plasma as a single fluid (Parker, 1957; Sweet, 1958; Petschek, 1964). The MHD framework is based on the

assumption that electrons and ions move together as a single fluid even in the presence of internal currents. This formulation has been reevaluated by a realization that the MHD condition does not always hold in a thin reconnection layer where ions become demagnetized and the relative drift velocity between electrons and ions can be large. This effect is considered to allow a large reconnection electric field at the reconnection region and is thus responsible for speeding up the rate of reconnection over Sweet-Parker rate. Generally speaking, two-fluid effects come into play due to the different behaviors of large orbit ions and strongly magnetized electrons [6]. Unfortunately, this approach is beyond the scope of the present Master thesis, which will be devoted to study the effect of Ohmic resistivity.

2. The Effect of Resistivity

The rate of MGR in the classical model of Sweet-Parker and Petscheck is proportional to plasma resistivity η , So by increasing the resistivity the rate of reconnection increases. But what physical interpretation could stand for such an increase in resistivity? And will numerical simulations agree with this suggestion?

In the work by Sweet-Parker (1958) and Petscheck (1964), the resistivity is taken to be uniform in space and constant in time. They attributed the resistivity to collisions between the electrons and ions, which causes the breakdown of the frozen-in condition of the plasma in the diffusion region. As we mentioned previously, these models assume ohmic resistivity and only one-fluid description. They lead to slow reconnection time scale as compared with the observations, for example in the solar corona. In Petscheck's model it is agreed that a narrow diffusion region accelerates the reconnection rate.

In this thesis, the main focus will be on studying the effect of resistivity as a main factor leading to an increase in the rate of magnetic reconnection which is presented in ChIII.

CHAPTER III

PRESENT CALCULATIONS OF MGR

A. Numerical Method

The equations of MHD presented in chap.II cannot be solved analytically. Thus, computational tools are the common way in plasma physics and fluid dynamics. The numerical treatment in the present work relies on a modern algorithm called **OpenFOAM**, an object-oriented library for Computational Fluid Dynamics (CFD) and structural analysis. Efficient and flexible implementation of complex physical models in Continuum Mechanics is achieved by mimicking the form of partial differential equation in software. The library provides Finite Volume and Finite Element discretisation in operator form and with polyhedral mesh support, with relevant auxiliary tools and support for massively parallel computing. Functionality of OpenFOAM is illustrated on three levels: improvements in linear solver technology with CG-AMG solvers, LES data analysis using Proper Orthogonal Decomposition (POD) and a self-contained fluid-structure interaction solver. [15]

Our main focus in the following is to investigate the role of resistivity in initiating the process of MGR. This is done by showing how the resistivity influences several relevant physical quantities. A self-consistent modeling of the resistivity is beyond the scope of the present work. Rather we use certain functional form that allows its variation over a large range as shown below. In order to achieve this goal we use the tools of OpenFOAM to solve the four equations (x, y, z, t) explained in Chap. II .

Following Wang et al. [16], we adopt a Gaussian-like functional form for the resistivity (η) appearing in the MHD equations, which is given by:

$$\eta = \eta_0 + \tilde{\eta} e^{-(x^2+y^2)} \quad (14)$$

where $\eta_0 = 1 \text{ } \Omega.m$ is the background resistivity and $\tilde{\eta}$ is the enhanced resistivity around the origin in order to vary it in the numerical simulations.

This functional form of η allows its spatial variation as a Gaussian distribution with a maximum given by $\tilde{\eta}$ which is varied as described below. It is emphasized that choosing this functional form of η allows its spatial variation as compared with a uniform distribution. It will be shown in the following that the maximum $\tilde{\eta}$ is the most crucial.

B. Initial and Boundary Conditions

To perform the numerical calculations, we proceed as follows:

- A two-dimensional domain is considered in the (x-y) plane with $x \in [-16 \delta, +16 \delta]$ and $y \in [-32 \delta, +32 \delta]$ with $\delta = 1.5 \times 10^6 \text{ m}$ is the half-width of the current layer.
- The numerical scheme consists of a non-uniform grid spacing being resolved with $5\mu\delta$ around the origin and with 0.3δ near the boundaries. The time step was chosen as $10ms$.
- Following the suggestion by [17], we assume an initial profile of the magnetic field with a y-component $B_y = B_0 \tanh(x)$. In addition, periodic boundary condition is used in the y-axis direction. As initial conditions, $T_0 = 2 \times 10^6 K$, $\rho_0 = 1.7 \times 10^{-9} \frac{g}{cm^3}$, and $v_0 = 0m/s$. Initial thermal pressure is obtained by solving equation of state ($p = (\gamma - 1)\rho e$), and magnetic pressure of value 0.1 Pascal is imposed at the boundary. Zero-gradient condition is used for velocity, magnetic field and Temperature.

C. Accuracy of the Numerical Program

In order to test the validity of the code and correctness of our simulation results figure (8) and (9) are shown. In figure (8), time evolution of the divergence of magnetic field \mathbf{B} for three cases of $\tilde{\eta}$ was varying between 10^{-24} and 10^{-19} Tesla which is compatible with zero. In figure (9) the residuals of three physical variables (temperature T , velocity \mathbf{u} , and magnetic field \mathbf{B}) shows 3 to 4 order of magnitude reduction. This indicates convergence and its less expected for the results to change as we continue running our code.

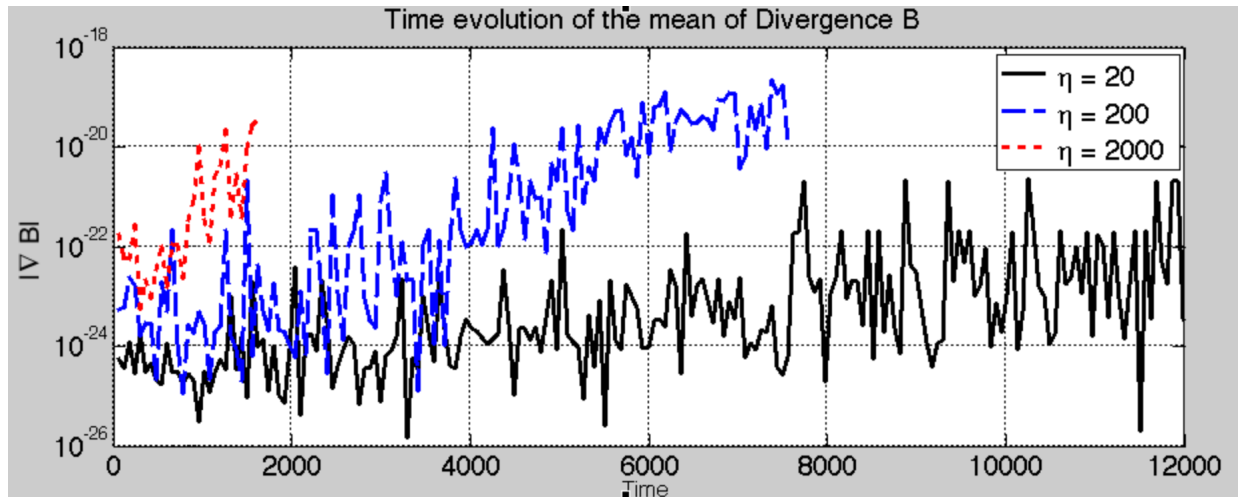


Figure 8: Time evolution of the divergence of magnetic field B during magnetic reconnection process at three different values of $\tilde{\eta}$ [time expressed in sec].

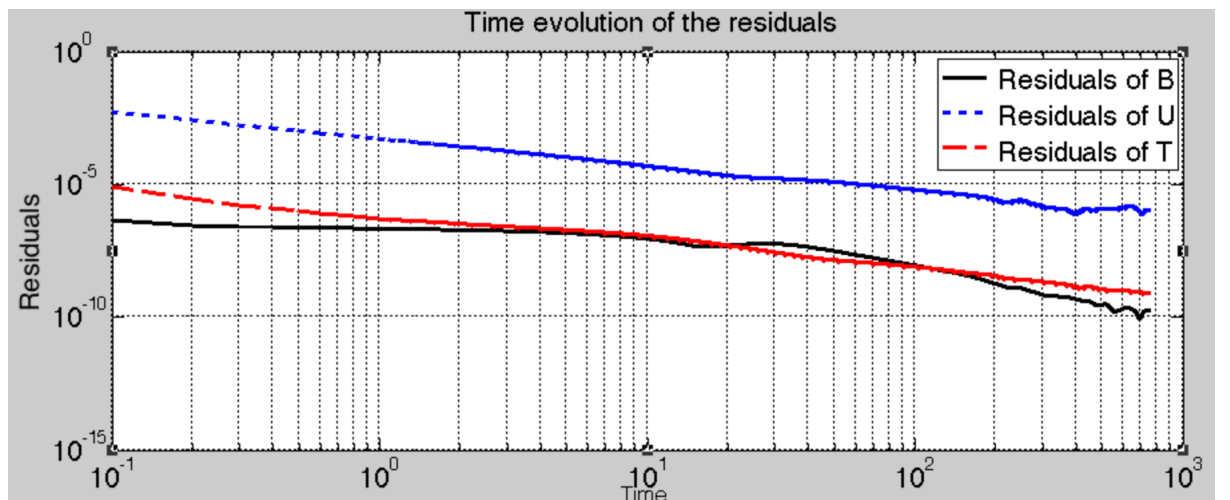


Figure 9: Time evolution of the residuals of magnetic field B , velocity U , and temperature T . [B expressed in Tesla, U in m/s, T in kelvins, and time in seconds].

D. Numerical Computations

Our focus in the present work is to study the effect of resistivity on the process of MGR as assumed above. We study the case where the initial conditions are taken to correspond to those associated with the solar corona.

We summarize the equations here again which are solved using the OpenFOAM algorithm.

Continuity equation

$$\frac{\partial \rho}{\partial t} + \nabla \cdot (\rho \mathbf{U}) = 0, \quad (15)$$

Momentum equation,

$$\frac{\partial (\rho \mathbf{U})}{\partial t} + \nabla \cdot (\rho \mathbf{U} \mathbf{U}) - \nu \Delta \mathbf{U} = -\nabla (p + \frac{B^2}{2\mu_0}) + \nabla \cdot (\frac{\mathbf{B}\mathbf{B}}{\mu_0}), \quad (16)$$

Induction equation

$$\frac{\partial \mathbf{B}}{\partial t} + \nabla \cdot (\mathbf{U}\mathbf{B}) - \frac{\eta}{\mu_0} \nabla^2 \mathbf{B} = \nabla \cdot (\mathbf{B}\mathbf{U}) + \mathbf{J} \times \nabla \eta, \quad (17)$$

Energy equation

$$\frac{\partial \rho E}{\partial t} + \nabla \cdot (\rho \mathbf{u} E) = -\nabla \cdot \left(\left(p + \frac{B^2}{2\mu_0} \right) \mathbf{u} \right) + \frac{1}{\mu_0} \nabla \cdot \left((\mathbf{B} \cdot \mathbf{u}) \mathbf{B} \right) - \frac{1}{\mu_0} \nabla \cdot (\eta \mathbf{j} \times \mathbf{B}) \quad (18)$$

where $E = e + \frac{1}{2}u^2 + \frac{B^2}{2\rho\mu_0}$ is the total energy of plasma per unit mass, e is the internal energy per unit mass, ρ is the plasma density ($\rho_0 = 1.7 \times 10^{-12} \text{ kg.m}^{-3}$ for hydrogen plasma), \mathbf{u} is the plasma velocity, \mathbf{B} is the magnetic field ($B_0 = 5 \text{ Gauss}$ is the typical magnetic field), and $\mu_0 = 4\pi \times 10^{-7} \text{ SI}$ is the permeability. Moreover, plasma is treated as an ideal gas, $p = (\gamma - 1)\rho e$. The functional form of resistivity as described above (see Eqn. 14).

E. Results of the Present Calculations

We present the results of a variety of calculations with different values of resistivity $\tilde{\eta}$.

1. Evolution of the Magnetic Field

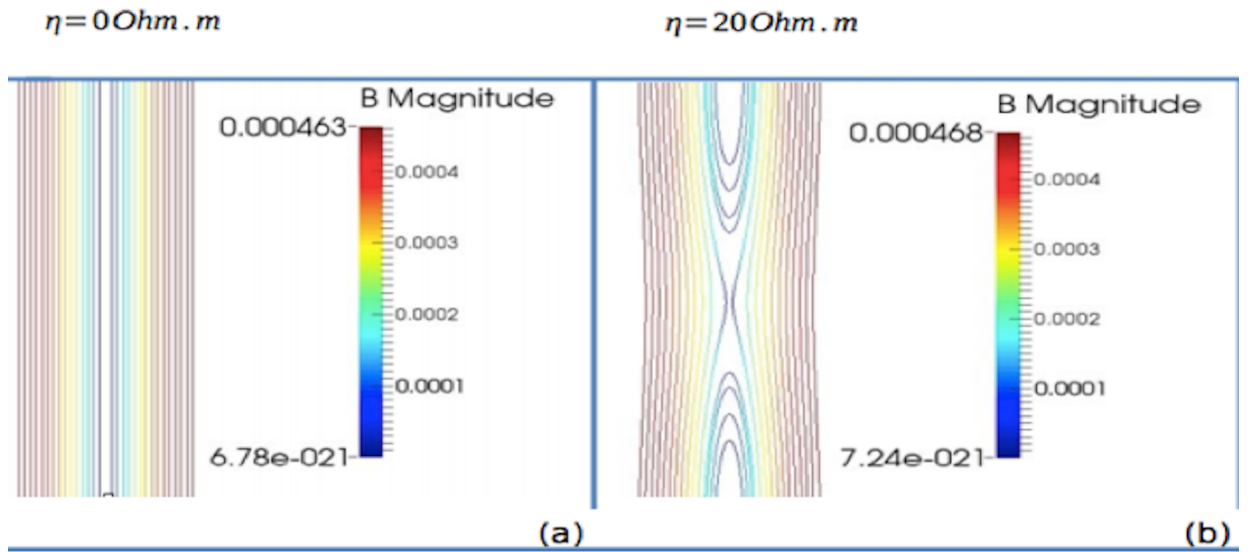


Figure 10: Result of the magnetic field evolution in case of $\eta = 0[\Omega.m]$ (left panel) and in case $\tilde{\eta} = 20[\Omega.m]$ (right panel) after a time of 200 min. Notice the development of magnetic reconnection in case of sapce dependent resistivity (right panel).

In the following we describe the time evolution of the magnetic field as its affected by the variation of the resistivity.

As expected, taking $\tilde{\eta} = 0$ did not lead to any MGR (see Fig10). In the case of finite $\eta = 20\Omega.m$ taken to be uniform MGR was not developed either. This means that in any model where resistivity should be included, it can not be uniform through the whole current sheet in order to lead to MGR.

This should not be confused with what was mentioned earlier in Chap.II (Sweet-Parker model with uniform resistivity). In fact it is hard to compare our results with those taken from Sweet and Parker (1958). As seen in Fig (5) the method used by S-P model defines

initially two regions, the whole current sheet with length $2L$ and then within it the diffusion region with length $2L$ but much narrower width 2δ , where resistivity is considered uniform inside the diffusion region and zero outside it. However, in our case we only defined length and width of the whole domain without setting any boundary for the diffusion region. So when we set η uniform, it means it's constant through the whole current sheet not only inside the diffusion region.

Indeed, MGR developed when the resistivity was taken to have a spatial dependence like a Gaussian distribution with $\tilde{\eta} = 20\Omega.m$ according to Eqn. (14). This is clearly seen in Fig (10-b), where the slingshot structure has shown up similar to what was described in connection with Fig(1) together with X-neutral point. However, remarkable in this case is the long time scale for the occurrence of MGR, which was at least 200 min. This is much longer than what was indicated by observation of the solar corona [12], which is only about 100 sec. Thus, one faces the challenge **not only to obtain MGR, but also as a relatively fast process**. This looks like the third mystery we have mentioned in the introduction.

The lesson here is that the development of MGR is too slow owing to the relatively small resistivity. Increasing the resistivity may lead to a faster reconnection time scale.

Taking $\tilde{\eta} = 200\Omega.m$ in Eq(14), resulted in the behavior shown in Fig(11), where several snapshots in time are shown. In particular, one sees how the current sheet becomes narrower in the course of time. The conclusion is that the MGR is faster but still not matching with the observations.

Taking $\tilde{\eta} = 2000\Omega.m$, we get the results shown in Fig(12). In this case, MGR develops after 5 min, and at 20 min two cusp-shaped magnetic islands are formed. The current sheet has become significantly thinner by time $t=25$ min.

In this section it was shown that magnetic reconnection requires some physical dissipation (effective resistivity $\tilde{\eta}$) to sustain its appearance at X-point. Hence, initiated by Gaussian disturbance assumed in Eqn(14), reconnection of magnetic field lines occurred while uni-

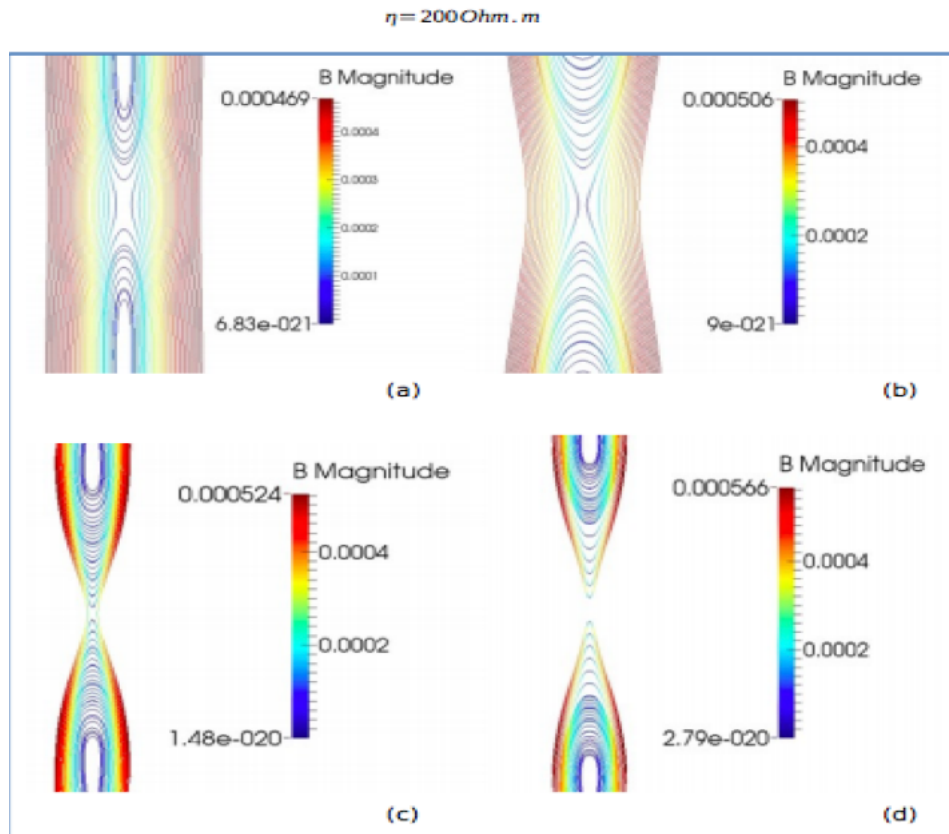


Figure 11: Stream lines of magnetic field B , expressed in Tesla, for case $\tilde{\eta} = 200 \Omega \cdot m$ at times (a) $t = 30$ min, (b) $t = 60$ min, (c) $t = 90$ min, (d) $t = 110$ min.

form resistivity model didn't show any evidence of MGR. Increasing then the maximum value of the resistivity ($\tilde{\eta}$) lead to faster reconnection time scale.

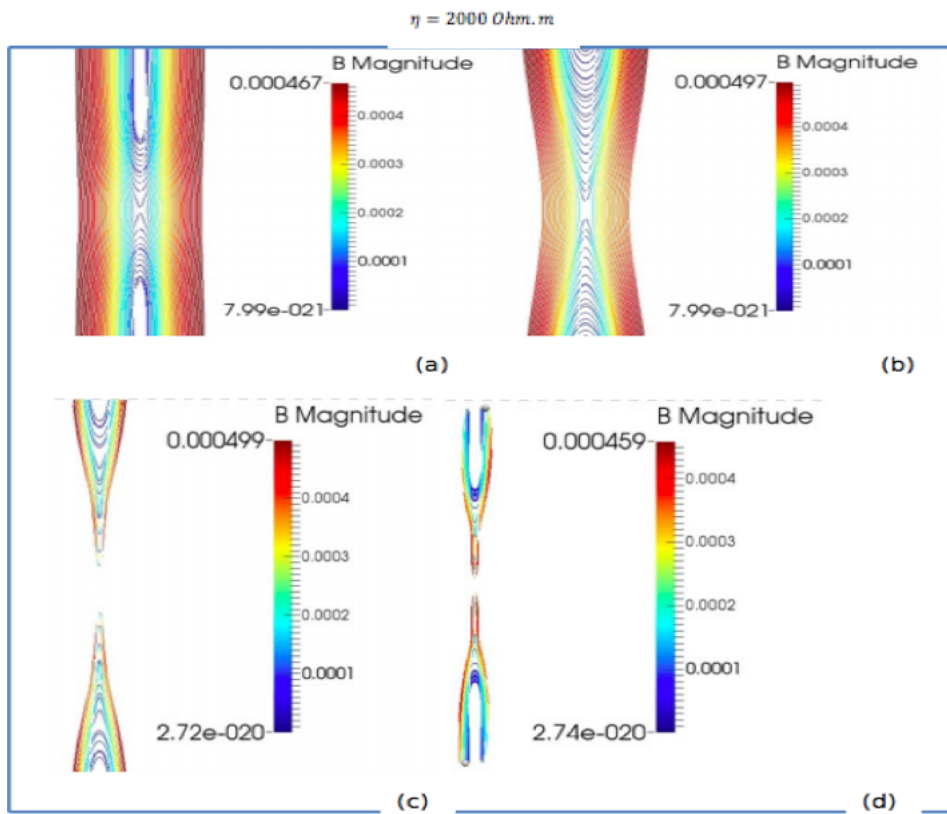


Figure 12: Stream lines of magnetic field B, expressed in Tesla, for case $\tilde{\eta} = 2000 \Omega.m$ at times: (a) $t = 5 \text{ min}$, (b) $t = 15 \text{ min}$, (c) $t = 20 \text{ min}$, (d) $t = 25 \text{ min}$.

2. Evolution of the Plasma Velocity

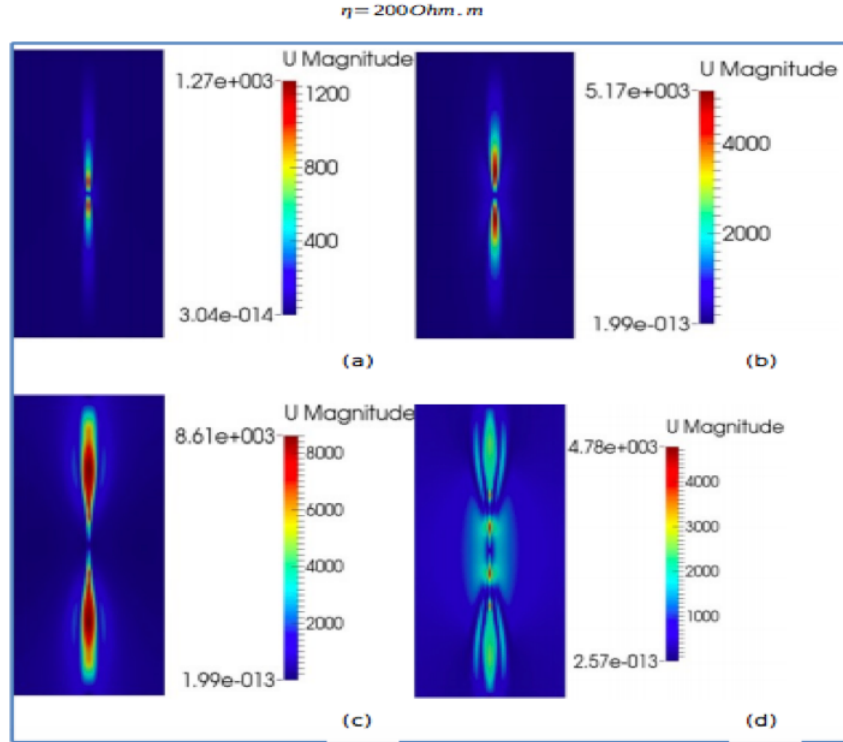


Figure 13: Velocity of plasma during magnetic reconnection, expressed in m/s, for case $\tilde{\eta} = 200 \Omega \cdot \text{m}$ at four different times (a) $t = 30$ min, (b) $t = 60$ min, (c) $t = 90$ min, (d) $t = 110$ min.

Figure (13) shows that the plasma velocity is vanishingly small near the center of the current sheet. As the plasma leaves the diffusion region an abruptly larger speed of the order of 10^3 m/s is achieved, which is consistent with the model of Petscheck [13], where it was argued that the plasma in the reconnection jet is compressed and changes its flow direction along the field and is accelerated by an enhanced gas pressure to become a pair of jets", and this is seen at time $t = 90$ min.

In Fig (14), where $\tilde{\eta} = 2000 \Omega \cdot \text{m}$ is adopted, the jet-like motion of the plasma is much faster and develop in about 15 min.

According to the model of Petscheck[13], it was argued that particles were expected to leave the diffusion region at speed approximately equal to Alfvén speed ($\sim 3 \times 10^4 \text{ m/s}$) [2]. In our calculation in the case $\tilde{\eta} = 2000 \Omega$, as shown in Fig (14), such high velocities are achieved only later in time like 25 min, despite the occurrence of MGR earlier at 5

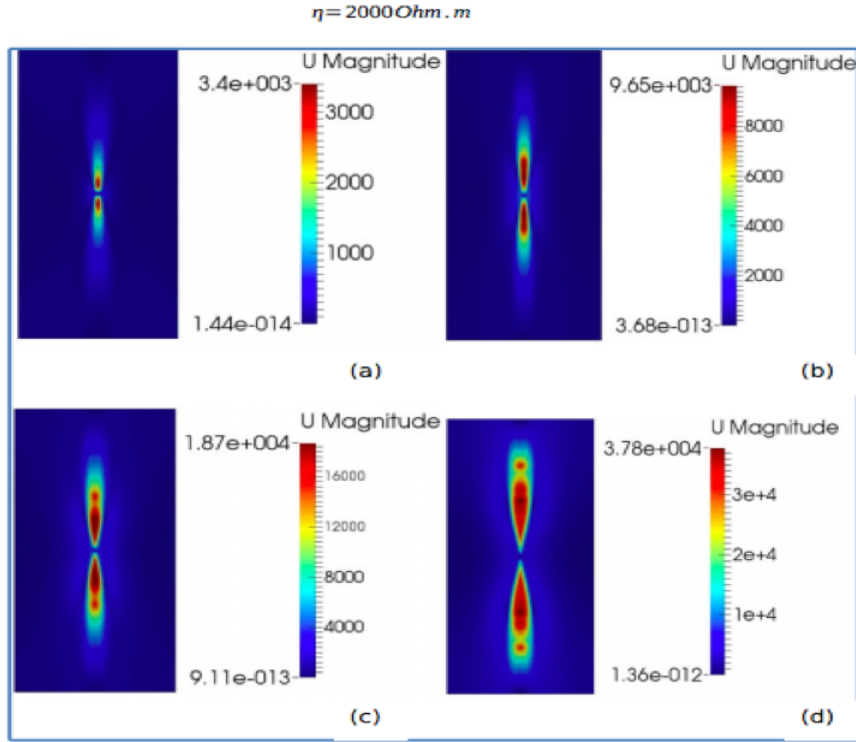


Figure 14: Velocity of plasma during magnetic reconnection, expressed in m/s, for case $\tilde{\eta} = 2000 \Omega \cdot m$ at four different times (a) $t = 5$ min, (b) $t = 15$ min, (c) $t = 20$ min, (d) $t = 25$ min.

min. A possible reason is that the Alfvén speed is detected after reconnection takes place between two jets, i.e. once magnetic island is formed, where the reconnection of magnetic field lines is not enough to reach these high speeds[18].

The learn effect of this part is : The results shown in figures (13 and 14) indicate that magnetic reconnection is shown to be a direct reason behind particle acceleration in space plasma.

3. Evolution of the Plasma Density

The value of resistivity has an indirect effect on the behavior of density during reconnection process. As presented in figures (15, 16 and 17) for two cases of $\tilde{\eta}=200$ and $2000 \Omega \cdot m$, it is seen that the density is shown to drop around the origin as plasma enters into the diffusion region.

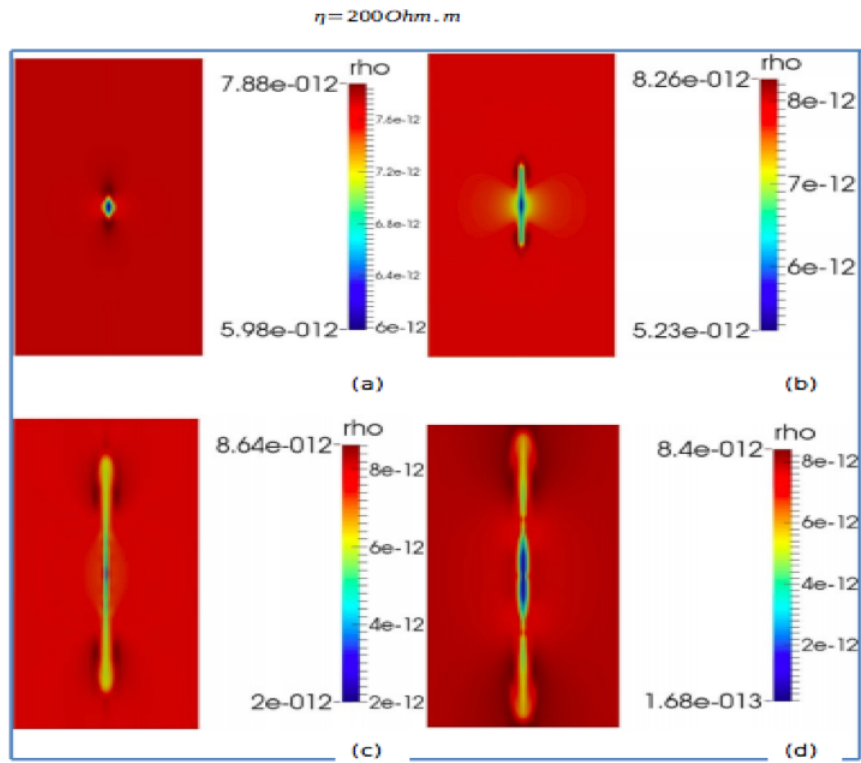


Figure 15: Density of plasma, expressed in kg.m^{-3} , for case $\tilde{\eta} = 200 \text{ } \Omega.\text{m}$ at four different times (a) $t = 30 \text{ min}$, (b) $t = 60 \text{ min}$, (c) $t = 90 \text{ min}$, (d) $t = 110 \text{ min}$.

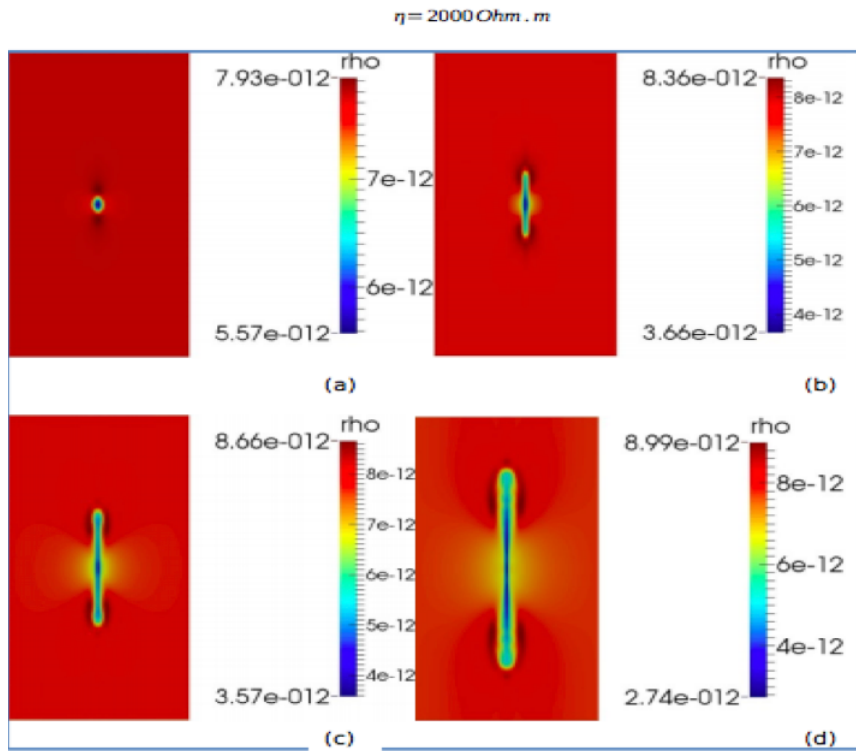
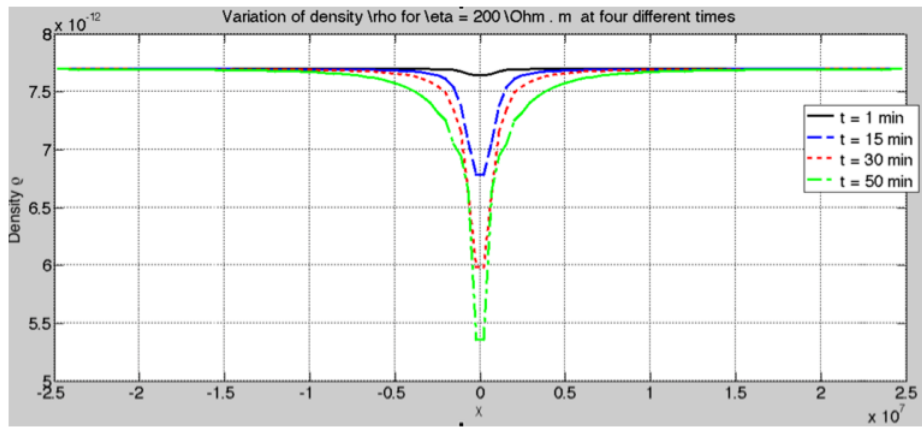
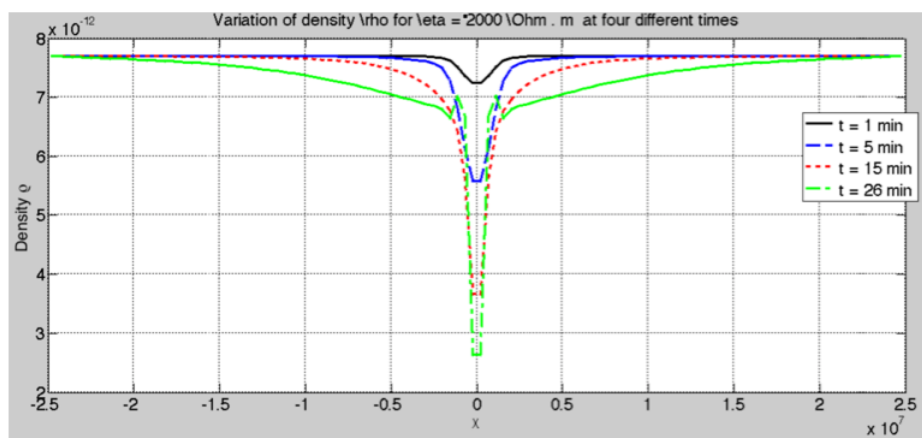


Figure 16: Density of plasma, expressed in kg.m^{-3} , for case $\tilde{\eta} = 2000 \text{ } \Omega.\text{m}$ at four different times (a) $t = 5 \text{ min}$, (b) $t = 15 \text{ min}$, (c) $t = 20 \text{ min}$, (d) $t = 25 \text{ min}$.



(a)



(b)

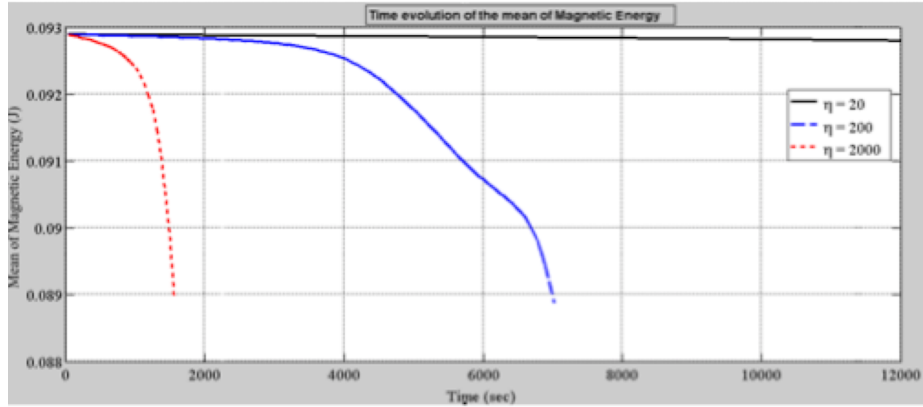
Figure 17: Variation of plasma Density in kg/m^3 as a function of the x -coordinate in meters for several times as indicated: (a) $\tilde{\eta} = 200 \text{ Ohm} \cdot \text{m}$, (b) $\tilde{\eta} = 2000 \text{ Ohm} \cdot \text{m}$

The Lorenz force drives plasma flows to reduce plasma density around the X -point and causes plasma inflow. At the center of the diffusion region, the plasma density is extremely reduced to enhance also the drift velocity as expected from previous section.

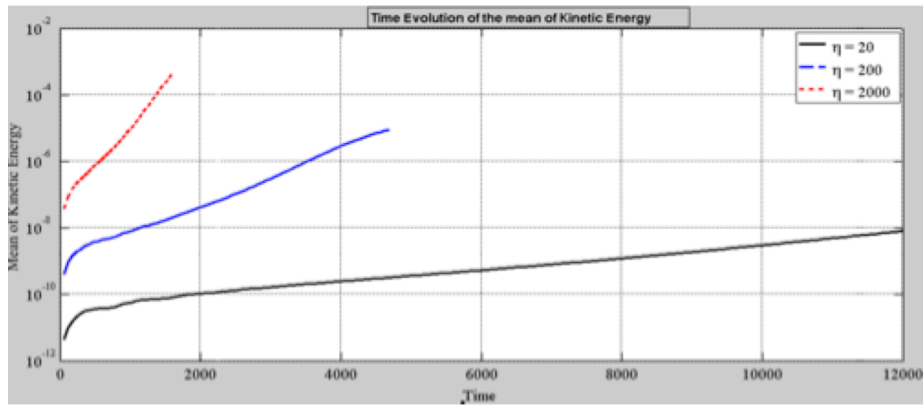
In case where $\tilde{\eta} = 2000 \Omega.m$, we noticed small increase in the density at time $t = 25$ min. This occurs at time $t = 25$ min when two magnetic jets were formed as seen in figure (12). This seems to be done due to reoccurrence of MGR.

It is interesting to notice that density cavity in the diffusion region was first noticed by Shay et al (2001)[19]. An observation of density cavity during reconnection process in a diffusion region in the presence of finite guide field was first detected by Øieroset (2001), and then by cluster spacecraft during reconnection at the magnetopause in March 2002 [19], see Fig (26).

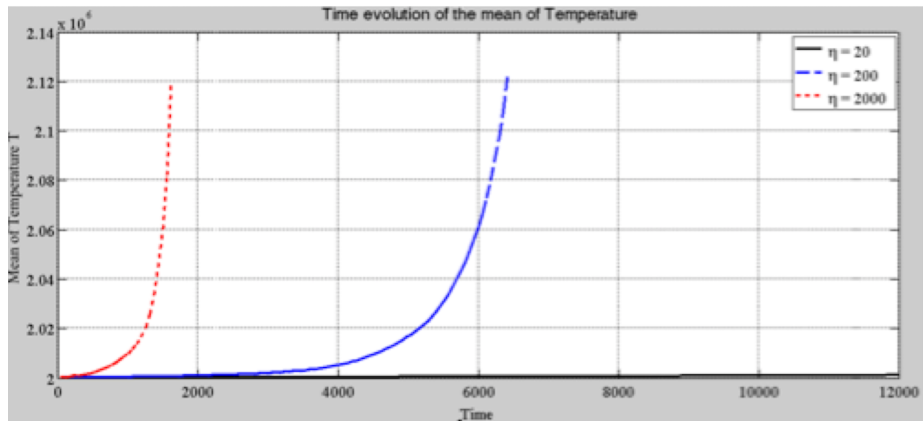
4. Evolution of Magnetic Energy, Temperature and Kinetic Energy



(a)



(b)



(c)

Figure 18: Time Evolution of the Mean of (a) Magnetic Energy, (b) Kinetic Energy and (c) Temperature of plasma during reconnection process for three values of $\tilde{\eta}$ ($\tilde{\eta} = 20, 200, \text{ and } 2000 \Omega.m$). Energy expressed in joules, temperature in kelvins, and time in seconds.

In figure (18 a-c), the evolution of the mean magnetic energy, the kinetic energy and the temperature is shown during the reconnection process. Magnetic energy is decreasing, while the kinetic energy and temperature increase as a function of time during the reconnection process.

As expected, no variation of these quantities is seen in case of $\tilde{\eta} = 20 \Omega.m$. In the other investigated cases, one can see the onset of reconnection, where the mean magnetic energy starts decreasing, while the kinetic energy and temperature are seen to increase. For example in Fig 18-c, these features are seen at an elapsed time of 1800 sec (30 min) indicating the onset of reconnection.

The higher value of $\tilde{\eta} = 2000 \Omega.m$ as in Fig (18-b) leads to faster onset of reconnection already at 300 sec (5 min).

The most important feature of magnetic reconnection is that significant acceleration and heating of plasma particles occurs at the expense of magnetic energy. More work is needed to see how magnetic reconnection leads to the heating of the solar corona from which the solar wind emerges.

5. Evolution of Reynold Number

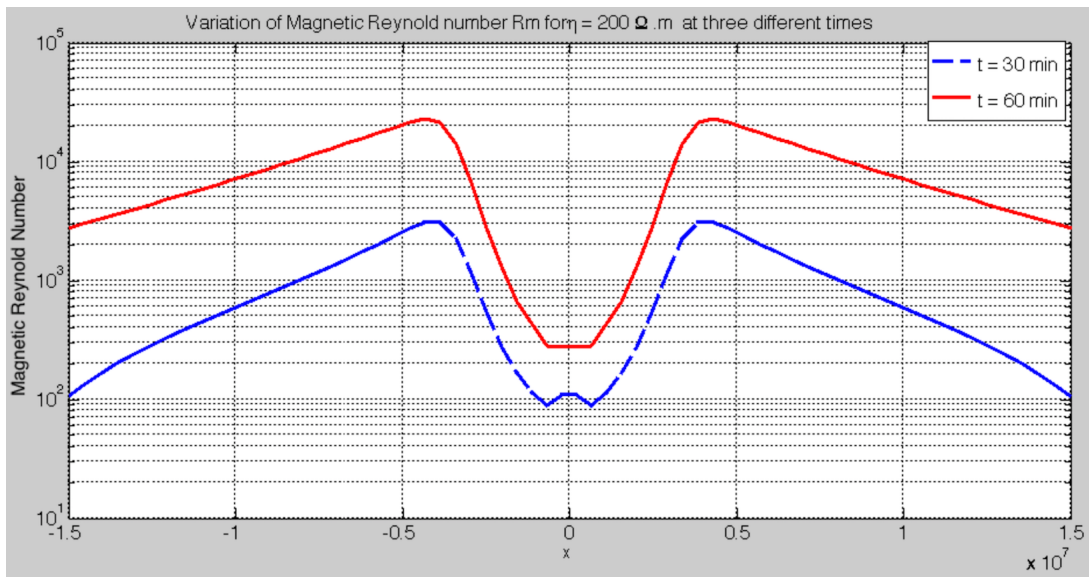


Figure 19: Variation of magnetic reynold number R_m inside the diffusion region for case $\tilde{\eta} = 200\Omega.m$ [x expressed in meters].

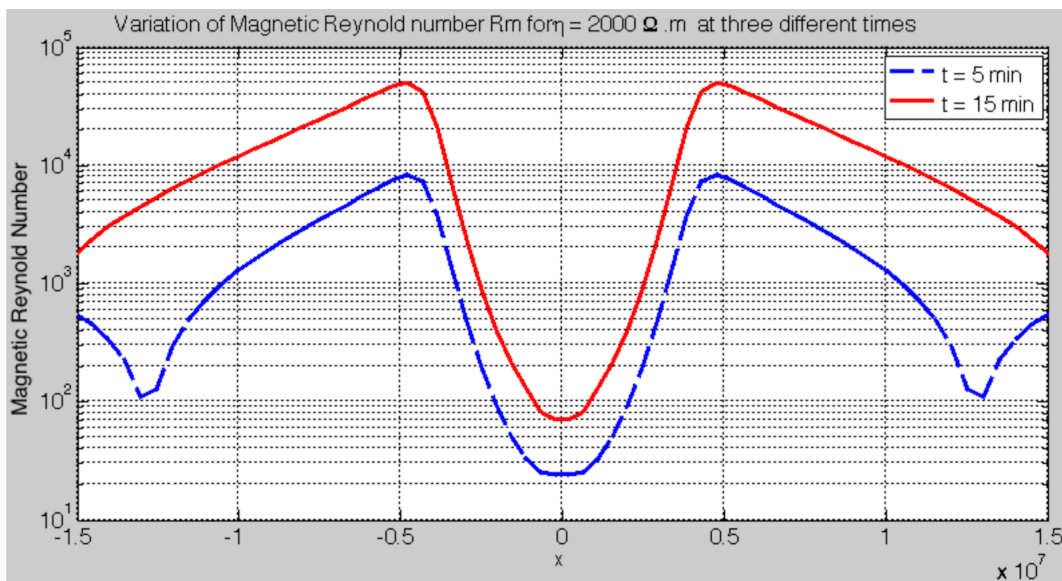


Figure 20: Variation of magnetic reynold number R_m inside the diffusion region for case $\tilde{\eta} = 2000\Omega.m$. [x expressed in meters].

Figures (19 and 20) shows variation of Magnetic Reynold number inside the diffusion region for two differnt values of resistivity ($\tilde{\eta} = 200\Omega.m$ and $\tilde{\eta} = 2000\Omega.m$). As expected in both figures the Reynold number is decreasing near the origin and it reaches a minimum value at center of the diffusion region where resistivity attains its maximum value.

For case of fast reconnection ($\tilde{\eta} = 2000\Omega.m$), $R_m \sim 10$ at the center of the diffusion region which is a very good value that allows annihilation of magnetic flux during MGR.

6. The Rate of Magnetic Reconnection Process

According to the Poynting flux theorem, magnetic reconnection requires an electric field \mathbf{E} that satisfies $\mathbf{E} \cdot \mathbf{J} > 0$ in the diffusion region, where $\mathbf{u} \times \mathbf{B}$ term is negligible, to provide physical dissipation. Also, Faraday's law indicates that the reconnection, or flux transfer rate should be defined as the electric field $|\mathbf{E}|$ measured at the X -point in the direction of \mathbf{J} , since the current density \mathbf{J} at the X -point is associated directly with the anti-parallel magnetic field component to be reconnected. Hence, the reconnection electric field \mathbf{E} should be given by $\eta\mathbf{J}$ at the X -point.

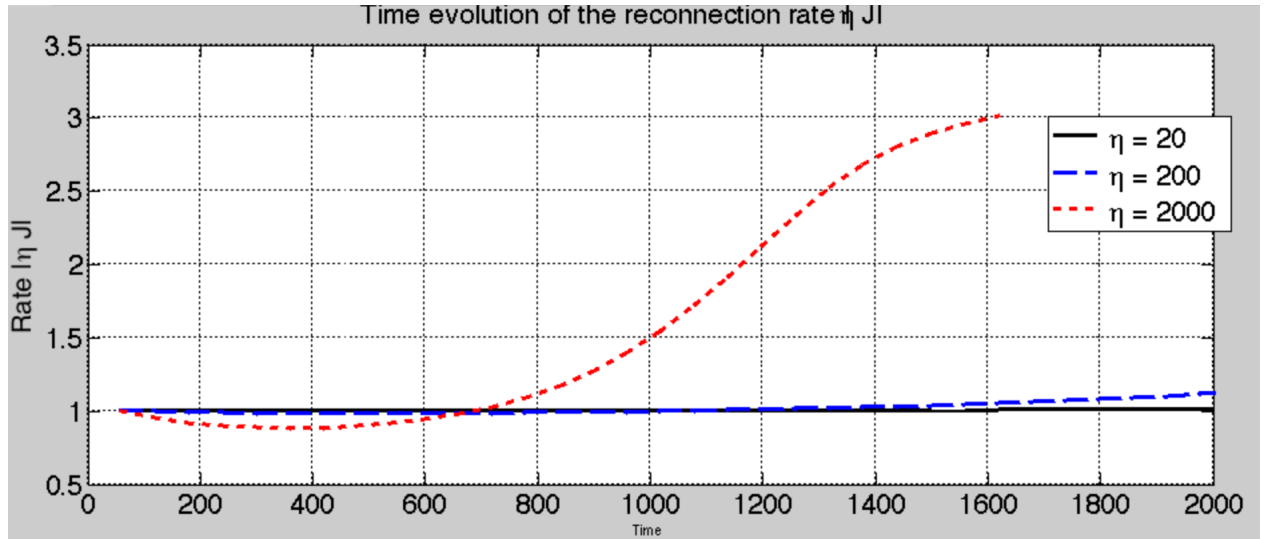


Figure 21: Rate of reconnection of plasma in the diffusion region versus time for three different cases of $\tilde{\eta}$. [time expressed in sec, η expressed in $\Omega.m$].

In fig (21), for case $\tilde{\eta}=20 \Omega.m$ as expected the rate did not show any difference as reconnection process is proceeding with time. For case $\tilde{\eta}=200 \Omega.m$ and by the time $t=1400$ sec the rate of reconnection starts to show slight increase with time. For case $\tilde{\eta}=2000 \Omega.m$

the rate of reconnection starts to increase beyond $t \sim 700$ sec which is must faster than the two previous cases. A small decrease in rate is witnessed before this time; this may be due to large dissipation effects localized in the diffusion region.

Notice that reconnection rate was much faster for case $\tilde{\eta} = 2000 \Omega.m$. We show then that the rate of reconnection is dependent on the value of resistivity of the plasma in the current sheet.

7. Effect of the size of the current sheet

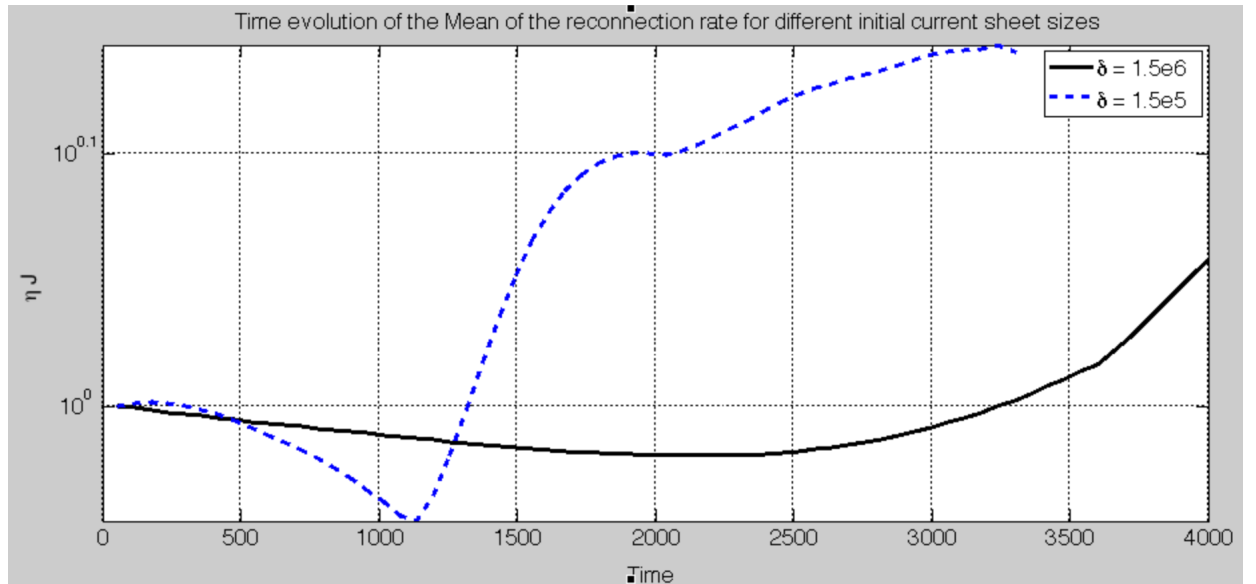


Figure 22: Rate of reconnection of plasma in the diffusion region versus time for two different values of current sheet width δ for case $\tilde{\eta} = 200 \Omega.m$. [time expressed in sec, δ expressed in m].

Figure (22) shows time evolution of rate of reconnection for different values of current sheet width δ for case $\tilde{\eta} = 200 \Omega.m$. Upon thinning the current sheet from value 1.5×10^6 to 1.5×10^5 m, reconnection is seen to launch much faster and the rate of reconnection increases rapidly. This result was expected because larger reconnection rate must be equivalent to larger electric field which requires smaller width ($E = \eta j = \frac{\eta B}{\mu \delta}$). We can then conclude that in addition to resistivity, the geometry of the current sheet plays an

important role in MGR process.

8. Effect of the initial Temperature

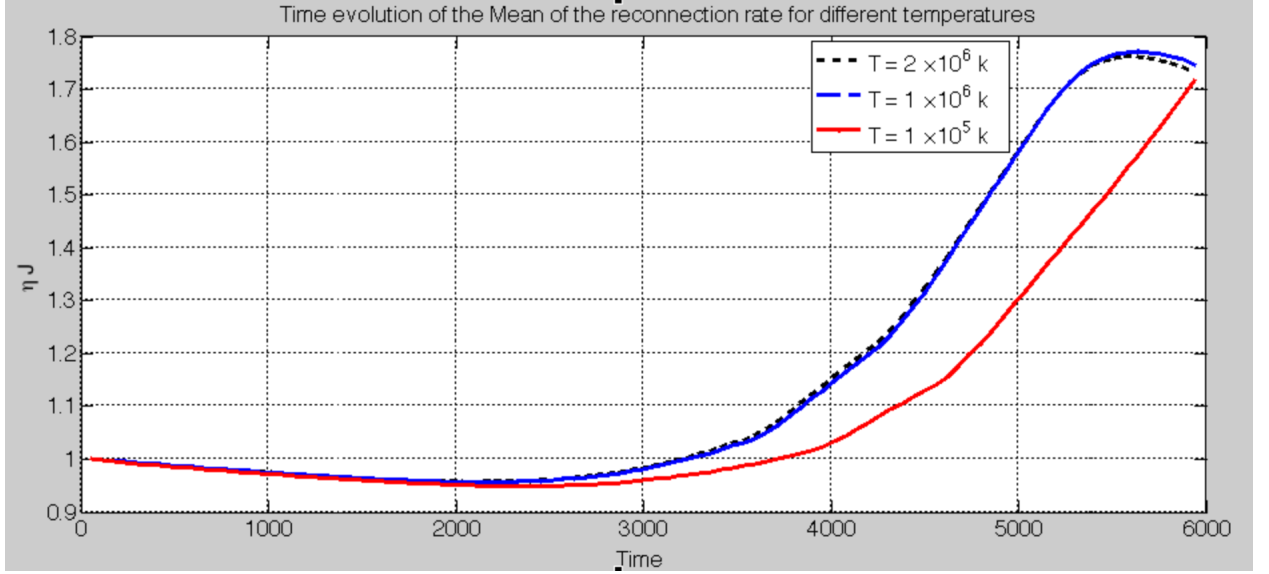


Figure 23: Rate of reconnection of plasma in the diffusion region versus time for three different values of initial temperature T for case $\tilde{\eta} = 200\Omega.m$. [time expressed in sec, T in Kelvin].

Figure (23) shows time evolution of reconnection rate for case $\tilde{\eta} = 200\Omega.m$ with three different initial temperatures T_i . Upon changing the initial temperature of the plasma from $T = 10^5 K$ to $T = 2 \times 10^6 K$ (temperature of the solar corona), the rate of reconnection has barely increased with time evolution. In our calculations (MHD model), the rate of reconnection $|E| = |\eta j|$, where η is space dependent and $j = \frac{\eta B}{\mu \delta}$. It is then expected that only $(B, \delta, \text{ and } \eta)$ will affect on the rate of reconnection. One may argue then why didn't we follow other temperature dependent resistivity suggestion.

In fact, the common temperature dependent resistivity distribution for one fluid model in space plasma is the Spitzer resistivity, which is due to Coulomb collisions with $\eta = \alpha [T(r,t)/T_0]^{-3/2}$. Adapting Spitzer resistivity model our code failed to develop MGR. In what follows we show results taken from (M.Ugai, 2012) [22] where he showed that

fast reconnection cannot evolve in any way through this model.

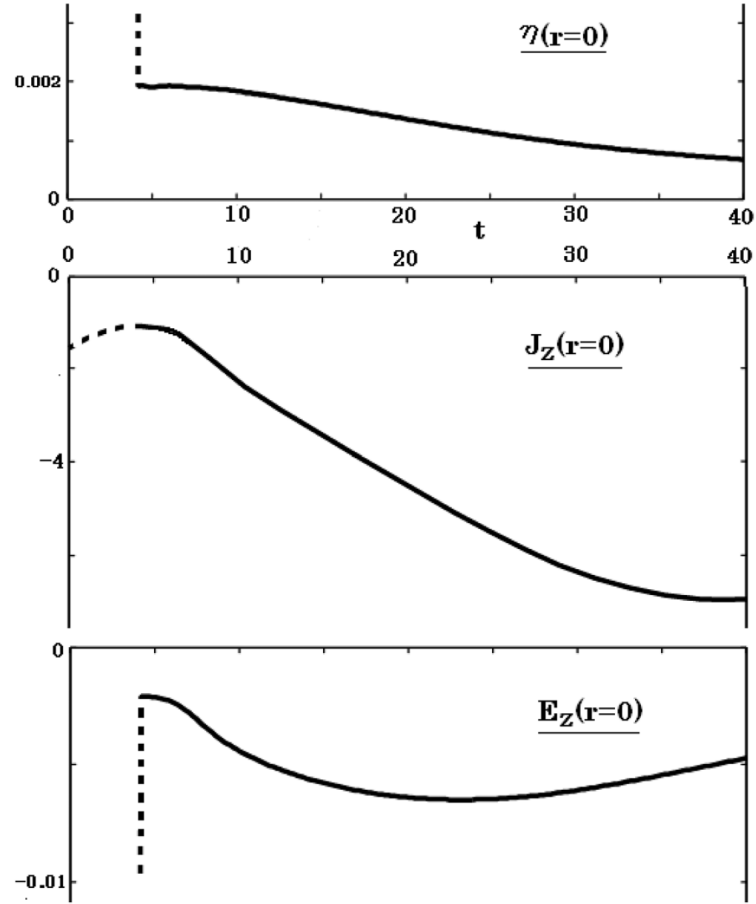


Figure 24: Temporal variations of resistivity η , current density J_z , and electric field E_z at the origin for the Spitzer resistivity model with $\alpha = 0.002$.

Fig (24) [22] shows the temporal behaviors of $\eta(r = 0)$, $J_z(r = 0)$, and $E_z(r = 0)$ measured at the X-point. Note that the resistivity around X-point reduces because of a temperature increase by Joule heating [22]. When resistivity becomes reduced, current density J is increasing due to thinning of the current sheet as discussed earlier in the previous section. Hence the reconnection rate $|E(r = 0)| = |\eta(r = 0)J(r = 0)|$ initially increases due to increase in $|J|$ but soon decreases because of the decrease in η .

It is shown then that unlike the Gaussian distribution we adopted earlier through this thesis (see Eqn (14)), Spitzer resistivity cannot grow MGR as resistivity becomes reduced

around X-point because of a sort of negative feedback.

It seems then that anomalous resistivity model that rises from momentum exchange between electrons and ions (two fluid model) should be included, but this is beyond the scope of this thesis.

F. Observations

In figures (25 [2] , 26 [19] , and 27 [21]) below we show observations detected by spacecrafts. Fig (25) shows coronal magnetic field lines while figures (26 and 27) show differnt physical quantities as observed during magnetic reconnection in Earth magnetopause. These figures serve as good candidates in order to understand the process of MGR.

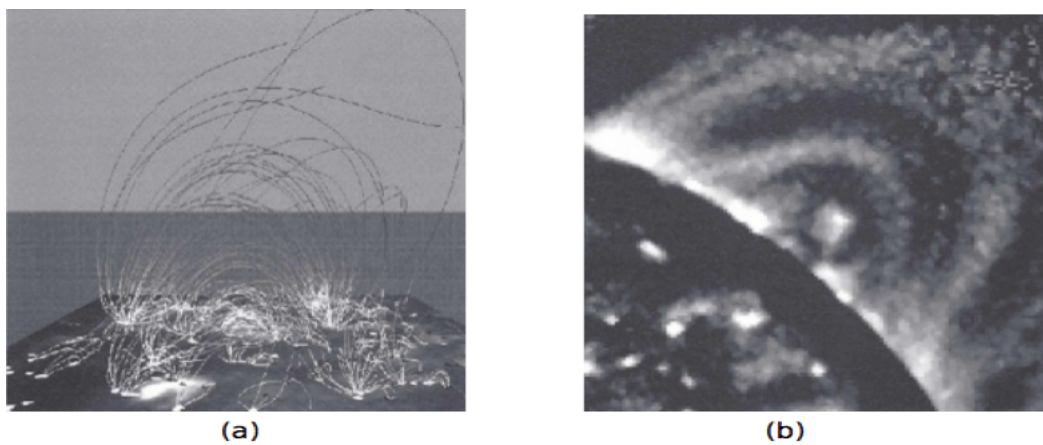


Figure 25: The so-called "magnetic carpet" showing observed photospheric magnetic fragments and overlying coronal magnetic field lines (courtesy of MDI consortium). (b) Image showing right corner of the global image of the sun in soft X-rays from the Japanese satellite Yohkoh.

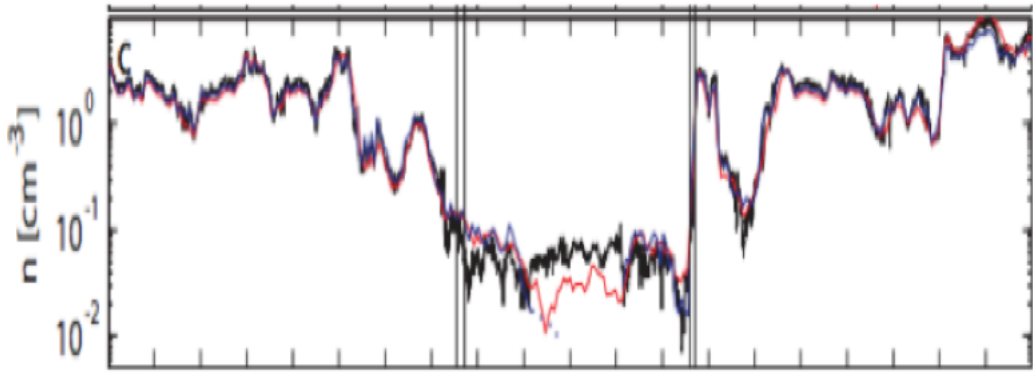


Figure 26: Density cavity observed on 13 March 2002 by Cluster spacecraft during reconnection process at the magnetopause.

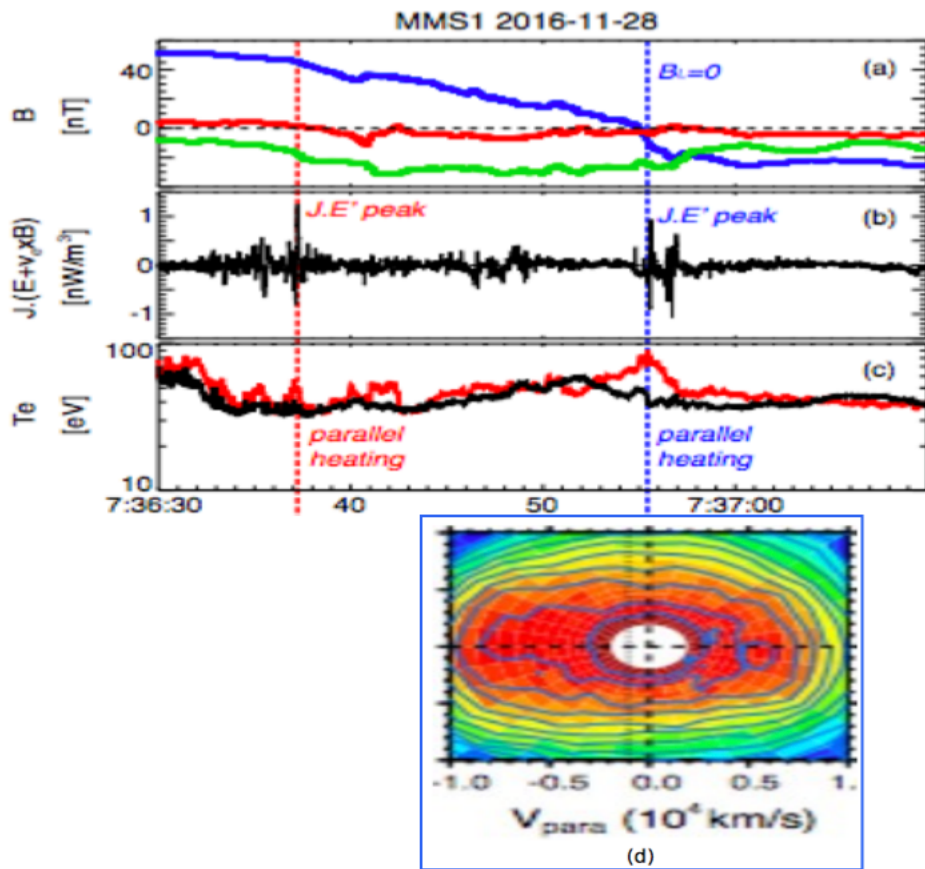


Figure 27: (a) magnetic field vector, (b) energy conversion rate in the electrons frame, (c) parallel (red) and perpendicular (black) electron temperature and (d) velocity of plasma for one event detected by MMS mission at 2016-11-28.

CHAPTER IV

CONCLUSION AND FUTURE WORK

This thesis has introduced basic magnetohydrodynamic model used to study magnetic reconnection process in stellar plasmas. We have presented the fundamental physics of magnetic reconnection discussing theoretical and numerical aspects, and summarizing observations.

In Chap.2 we presented the basic equations of a single fluid as they are needed to describe magnetic reconnection through combination of the fluid equations with the Maxwell equations of electromagnetism. We have followed the framework of two traditional works by Sweet and Parker (1958) and Petscheck (1964) describing the connection between the resistivity and magnetic reconnection. Guided with these ideas we have made some effort to pin down the effect of resistivity in initiating magnetic reconnection. We adapted a Gaussian space dependant resistivity model and then included the energy equation with the hope that our investigation will be more physical and may help to understand for example what is happening in the solar corona. We have also tested the effect of modification of the size of current sheet and initial temperature on the rate of reconnection.

In Chap.3, we have summarized our results with variable resistivity. Our results are summarized as follows.

- (a) Zero or spatially uniform resistivity does not lead to any MGR.
- (b) Assuming a Gaussian resistivity distribution (see Eq.14) with a variable maximum leads to MGR as seen in Chap.3. The reconnection time scale turns out to be rather sensitive to the adopted maximum of the Gaussian distribution, but not sensitive to spatial profile.

(c) Topological restructuring of magnetic field lines takes place as shown in figures (10,11, and 12) where field lines break and reconnect as they diffuse near the center forming X-type neutral point with zero magnetic field at the center. The plasma velocity becomes rather high after reconnection of the field lines. Achieving a velocity comparable to the Alfven velocity ($\sim 3 \times 10^4 m/s$) was only reached later after the occurrence of reconnection and with $\tilde{\eta} = 2000\Omega.m$. The plasma density was found to drop in the diffusion region in order to enhance the drift velocity. These investigations show that MGR accelerates the plasma particles, and the dropping in the magnetic energy was converted into kinetic and thermal energy. For this reason, MGR is a favored model for the heating of solar corona.

(d) Most remarkable effect of enhanced resistivity is its influence on the time scale of reconnection. This is clearly shown in figure (21). However, as shown in figure (22), the time scale of reconnection is strongly modified by reducing the width of the current sheet. Thus one cannot actually determine the reconnection rate without talking about the geometry of the diffusion region.

(e) Varying the initial temperature does not lead to a remarkable change in the rate of reconnection. Effect of temperature should be related to the temperature dependence of resistivity which was not done. The most crucial point is to include anomalous resistivity or a non-ohmic resistivity.

From the investigations in the present work, one learns that MGR cannot occur in a plasma described by ideal MHD. Also a single fluid model treating ions and electrons together is not a realistic model. A two fluid modeling seems necessary (M.Hamoud, private communication).

An elaborated modeling of MGR as occurring in the Sun's corona should be able to follow the transition from high Reynolds number to a lower one in a self-consistent way.

Our effort in this thesis is in support of this view, and we have successfully tested the numerical simulations and got more insight in the process of MGR.

BIBLIOGRAPHY

- [1] Alessandro Retinò. *Magnetic Reconnection in Space Plasmas: Cluster Spacecraft Observations*. PhD thesis, Acta Universitatis Upsaliensis, 2007.
- [2] E Priest and T Forbes. *Magnetic reconnection: Mhd theory and applications* cambridge univ. Press, Cambridge, 2000.
- [3] Russell M Kulsrud. Magnetic reconnection in a magnetohydrodynamic plasma. *Physics of Plasmas*, 5(5):1599–1606, 1998.
- [4] Russell M Kulsrud. Important plasma problems in astrophysics. *Physics of Plasmas*, 2(5):1735–1745, 1995.
- [5] C Litwin, Edward F Brown, and R Rosner. Ballooning instability in polar caps of accreting neutron stars. *The Astrophysical Journal*, 553(2):788, 2001.
- [6] Masaaki Yamada, Russell Kulsrud, and Hantao Ji. Magnetic reconnection. *Reviews of Modern Physics*, 82(1):603, 2010.
- [7] SI Syrovatsky. Particle acceleration and plasma ejection from the sun. In *Solar-Terrestrial Physics/1970*, pages 119–133. Springer, 1972.
- [8] JL Burch, TE Moore, RB Torbert, and BL Giles. Magnetospheric multiscale overview and science objectives. *Space Science Reviews*, 199(1-4):5–21, 2016.

- [9] Carolus J Schrijver and George L Siscoe. *Heliophysics: Plasma Physics of the Local Cosmos*. Cambridge University Press, 2009.
- [10] Robert T Glassey. *The Cauchy problem in kinetic theory*. SIAM, 1996.
- [11] Dieter Biskamp. Magnetic reconnection in plasmas. *Astrophysics and Space Science*, 242(1-2):165–207, 1996.
- [12] *Sweet-Parker Reconnection with Anomalous Resistivity? A Toy Model*, 2010.
- [13] Russell M Kulsrud. Magnetic reconnection: Sweet-parker versus petschek. *Earth, Planets and Space*, 53(6):417–422, 2001.
- [14] Kyōji Nishikawa and Masahiro Wakatani. *Plasma Physics: basic theory with fusion applications*, volume 8. Springer Science & Business Media, 2013.
- [15] Hrvoje Jasak, Aleksandar Jemcov, Zeljko Tukovic, et al. Openfoam: A c++ library for complex physics simulations. In *International workshop on coupled methods in numerical dynamics*, volume 1000, pages 1–20. IUC Dubrovnik, Croatia, 2007.
- [16] LC Wang, LJ Li, ZW Ma, X Zhang, and LC Lee. Energy of alfvén waves generated during magnetic reconnection. *Physics Letters A*, 379(36):2068–2072, 2015.
- [17] *Effect of magnetic reconnection in stellar plasma*, 2017.
- [18] Takaaki Yokoyama and Kazunari Shibata. Magnetic reconnection as the origin of x-ray jets and halpha surges on the sun. *Nature*, 375(6526):42, 1995.
- [19] M Zhou, Y Pang, XH Deng, ZG Yuan, and SY Huang. Density cavity in magnetic reconnection diffusion region in the presence of guide field. *Journal of Geophysical Research: Space Physics*, 116(A6), 2011.
- [20] Säm Krucker, HS Hudson, L Glesener, SM White, S Masuda, J-P Wuelser, and RP Lin. Measurements of the coronal acceleration region of a solar flare. *The Astrophysical Journal*, 714(2):1108, 2010.

